

**Mitochondrial respiratory states and rates:  
Building blocks of mitochondrial physiology  
Part 1.**

[http://www.mitoeagle.org/index.php/MitoEAGLE\\_preprint\\_2018-02-08](http://www.mitoeagle.org/index.php/MitoEAGLE_preprint_2018-02-08)

Preprint version 26 (2018-02-18)

**MitoEAGLE Network**

Corresponding author: Gnaiger E

Contributing co-authors

Acuna-Castroviejo D, Ahn B, Alves MG, Amati F, Aral C, Arandarčikaitė O, Åsander  
Frostner E, Bailey DM, Bastos Sant'Anna Silva AC, Battino M, Beard DA, Ben-Shachar D,  
Bishop D, Borutaitė V, Breton S, Brown GC, Brown RA, Buettner GR, Burtscher J, Calabria  
E, Cardoso LHD, Carvalho E, Casado Pinna M, Cervinkova Z, Chang SC, Chen Q, Chicco  
AJ, Chinopoulos C, Coen PM, Collins JL, Crisóstomo L, Davis MS, Dias T, Distefano G,  
Doerrier C, Drahota Z, Duchon MR, Ehinger J, Elmer E, Endlicher R, Fell DA, Ferko M,  
Ferreira JCB, Filipovska A, Fisar Z, Fisher J, Garcia-Roves PM, Garcia-Souza LF, Genova  
ML, Gonzalo H, Goodpaster BH, Gorr TA, Grefte S, Han J, Harrison DK, Hellgren KT,  
Hernansanz P, Holland O, Hoppel CL, Houstek J, Hunger M, Iglesias-Gonzalez J, Irving BA,  
Iyer S, Jackson CB, Jadiya P, Jansen-Dürr P, Jespersen NR, Jha RK, Kaambre T, Kane DA,  
Kappler L, Karabatsiakakis A, Keijer J, Keppner G, Komlodi T, Kopitar-Jerala N, Krako  
Jakovljevic N, Kuang J, Kucera O, Labieniec-Watala M, Lai N, Laner V, Larsen TS, Lee HK,  
Lemieux H, Lerfall J, Lucchinetti E, MacMillan-Crow LA, Makrecka-Kuka M, Meszaros AT,  
Michalak S, Moiso N, Molina AJA, Montaigne D, Moore AL, Moreira BP, Mracek T,  
Muntane J, Muntean DM, Murray AJ, Nedergaard J, Nemec M, Newsom S, Nozickova K,  
O'Gorman D, Oliveira PF, Oliveira PJ, Orynbayeva Z, Pak YK, Palmeira CM, Patel HH,  
Pecina P, Pereira da Silva Grilo da Silva F, Pesta D, Petit PX, Pichaud N, Pirkmajer S, Porter  
RK, Pranger F, Prochownik EV, Puurand M, Radenkovic F, Reboredo P, Renner-Sattler K,  
Robinson MM, Rohlena J, Røslund GV, Rossiter HB, Rybacka-Mossakowska J, Saada A,  
Salvadego D, Scatena R, Schartner M, Scheibye-Knudsen M, Schilling JM, Schlattner U,  
Schoenfeld P, Schwarzer C, Scott GR, Shabalina IG, Sharma P, Shevchuk I, Siewiera K,  
Singer D, Sobotka O, Sokolova I, Spinazzi M, Stankova P, Stier A, Stocker R, Sumbalova Z,  
Suravajhala P, Tanaka M, Tandler B, Tepp K, Tomar D, Towheed A, Tretter L, Trivigno C,  
Tronstad KJ, Trougakos IP, Tyrrell DJ, Urban T, Valentine JM, Velika B, Vendelin M,  
Vercesi AE, Victor VM, Villena JA, Wagner BA, Ward ML, Watala C, Wei YH, Wieckowski  
MR, Wohlgend M, Wolff J, Wuest RCI, Zaugg K, Zaugg M, Zorzano A

Supporting co-authors:

Bakker BM, Bernardi P, Boetker HE, Borsheim E, Bouitbir J, Calbet JA, Calzia E, Chaurasia  
B, Clementi E, Coker RH, Collin A, Das AM, De Palma C, Dubouchaud H, Durham WJ,  
Dyrstad SE, Engin AB, Fischer M, Fornaro M, Gan Z, Garlid KD, Garten A, Gourlay CW,  
Granata C, Haas CB, Haavik J, Haendeler J, Hand SC, Hepple RT, Hickey AJ, Hoel F, Jang  
DH, Kainulainen H, Khamoui AV, Klingenspor M, Koopman WJH, Kowaltowski AJ,  
Krajcova A, Lane N, Lenaz G, Liu J, Liu SS, Malik A, Markova M, Mazat JP, Menze MA,  
Methner A, Neuzil J, Oliveira MT, Pallotta ML, Parajuli N, Pettersen IK, Porter C,  
Pulinilkunnil T, Ropelle ER, Salin K, Sandi C, Sazanov LA, Silber AM, Skolik R, Smenes  
BT, Soares FAA, Sonkar VK, Swerdlow RH, Szabo I, Trifunovic A, Thyfault JP, Vieyra A,  
Votion DM, Williams C, Zischka H

## Updates and discussion:

[http://www.mitoeagle.org/index.php/MitoEAGLE\\_preprint\\_2018-02-08](http://www.mitoeagle.org/index.php/MitoEAGLE_preprint_2018-02-08)

Correspondence: Gnaiger E

Chair COST Action CA15203 MitoEAGLE – <http://www.mitoeagle.org>

Department of Visceral, Transplant and Thoracic Surgery, D. Swarovski Research  
Laboratory, Medical University of Innsbruck, Innrain 66/4, A-6020 Innsbruck, Austria

Email: erich.gnaiger@i-med.ac.at

Tel: +43 512 566796, Fax: +43 512 566796 20

## Contents

### Abstract

### Executive summary

### 1. Introduction – Box 1: In brief: Mitochondria and Bioblasts

### 2. Oxidative phosphorylation and coupling states in mitochondrial preparations

Mitochondrial preparations

#### 2.1. Respiratory control and coupling

The steady-state

Specification of biochemical dose

Phosphorylation,  $P_{\gg}$ , and  $P_{\gg}/O_2$  ratio

Control and regulation

Respiratory control and response

Respiratory coupling control and ET-pathway control

Coupling

Uncoupling

#### 2.2. Coupling states and respiratory rates

Respiratory capacities in coupling control states

LEAK, OXPHOS, ET, ROX

#### 2.3. Classical terminology for isolated mitochondria

States 1–5

### 3. Normalization: fluxes and flows

#### 3.1. Normalization: system or sample

Flow per system,  $I$

Extensive quantities

Size-specific quantities – Box 2: Metabolic fluxes and flows: vectorial and scalar

#### 3.2. Normalization for system-size: flux per chamber volume

System-specific flux,  $J_{V,O_2}$

#### 3.3. Normalization: per sample

Sample concentration,  $C_{mX}$

Mass-specific flux,  $J_{O_2/mX}$

Number concentration,  $C_{NX}$

Flow per object,  $I_{O_2/X}$

#### 3.4. Normalization for mitochondrial content

Mitochondrial concentration,  $C_{mtE}$ , and mitochondrial markers

Mitochondria-specific flux,  $J_{O_2/mtE}$

#### 3.5. Evaluation of mitochondrial markers

#### 3.6. Conversion: units

### 4. Conclusions – Box 3: Mitochondrial and cell respiration

### 5. References

**Abstract** As the knowledge base and importance of mitochondrial physiology to human health expand, the necessity for harmonizing nomenclature concerning mitochondrial respiratory states and rates has become increasingly apparent. Clarity of concept and consistency of nomenclature are key trademarks of a research field. These trademarks facilitate effective transdisciplinary communication, education, and ultimately further discovery. Peter Mitchell's chemiosmotic theory establishes the mechanism of energy transformation and coupling in oxidative phosphorylation. The unifying concept of the protonmotive force provides the framework for developing a consistent theory and nomenclature for mitochondrial physiology and bioenergetics. Herein, we follow IUPAC guidelines on general terms of physical chemistry, extended by considerations on open systems and irreversible thermodynamics. We align the nomenclature and symbols of classical bioenergetics with a concept-driven constructive terminology to express the meaning of each quantity clearly and consistently. In this position statement, in the frame of COST Action MitoEAGLE, we endeavour to provide a balanced view on mitochondrial respiratory control and a critical discussion on reporting data of mitochondrial respiration in terms of metabolic flows and fluxes. Uniform standards for evaluation of respiratory states and rates will ultimately support the development of databases of mitochondrial respiratory function in species, tissues, and cells.

*Keywords:* Mitochondrial respiratory control, coupling control, mitochondrial preparations, protonmotive force, oxidative phosphorylation, OXPHOS, efficiency, electron transfer, ET; proton leak, LEAK, residual oxygen consumption, ROX, State 2, State 3, State 4, normalization, flow, flux

---

## Executive summary

1. In view of broad implications on health care, mitochondrial researchers face an increasing responsibility to disseminate their fundamental knowledge and novel discoveries to a wide range of stakeholders and scientists beyond the group of specialists. This requires implementation of a commonly accepted terminology within the discipline and standardization in the translational context. Authors, reviewers, journal editors, and lecturers are challenged to collaborate with the aim to harmonize the nomenclature in the growing field of mitochondrial physiology and bioenergetics.
2. Aerobic energy metabolism in mammalian mitochondria depends on the coupling of ADP → ATP phosphorylation to oxygen consumption in catabolic reactions. In this process of oxidative phosphorylation, coupling is mediated by translocation of protons through respiratory proton pumps operating across the inner mitochondrial membrane and generating or utilizing the protonmotive force measured between the mitochondrial matrix and intermembrane compartment. Compartmental coupling thus distinguishes vectorial oxidative phosphorylation from fermentation as the counterpart of cellular core energy metabolism.
3. To exclude fermentation and other cytosolic interactions from exerting an effect on mitochondrial metabolism, the barrier function of the plasma membrane must be disrupted. Selective removal or permeabilization of the plasma membrane yields mitochondrial preparations—including isolated mitochondria, tissue and cellular preparations—with structural and functional integrity. Then extra-mitochondrial concentrations of fuel substrates transported into the mitochondrial matrix, ADP, ATP, inorganic phosphate, and cations including H<sup>+</sup> can be controlled to determine mitochondrial function under a set of conditions defined as coupling control states.

A concept-driven terminology of bioenergetics incorporates in its terms and symbols explicitly information on the nature of respiratory states, that makes the technical terms readily recognized and easy to understand.

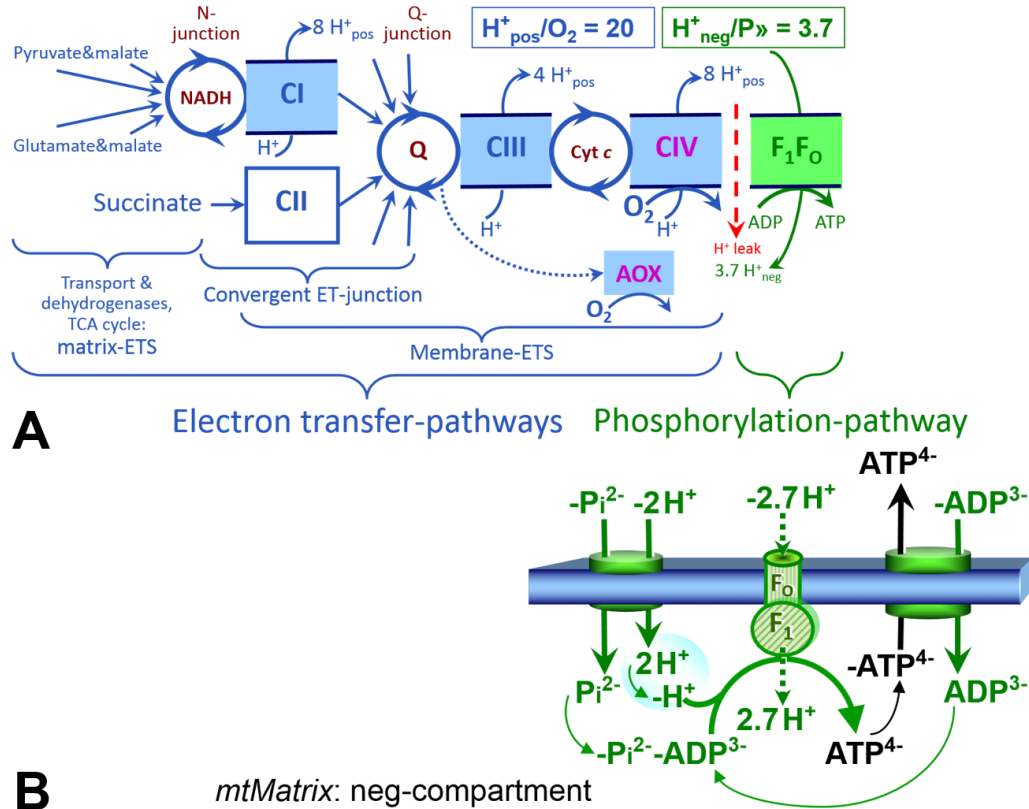


**Fig. 1. The oxidative phosphorylation (OXPHOS) system.** (A) The mitochondrial electron transfer system (ETS) is fuelled by diffusion and transport of substrates across the mtOM and mtIM and consists of the matrix-ETS and membrane-ETS. ET-pathways are coupled to the phosphorylation-pathway. ET-pathways converge at the N-junction and Q-junction. Additional arrows indicate electron entry into the Q-junction through electron transferring flavoprotein, glycerophosphate dehydrogenase, dihydro-orotate dehydrogenase, choline dehydrogenase, and sulfide-ubiquinone oxidoreductase. The dotted arrow indicates the branched pathway of oxygen consumption by alternative quinol oxidase (AOX). The  $H^+_{pos}/O_2$  ratio is the outward proton flux from the matrix space to the positively (pos) charged compartment, divided by catabolic  $O_2$  flux in the NADH-pathway. The  $H^+_{neg}/P$  ratio is the inward proton flux from the inter-membrane space to the negatively (neg) charged matrix space, divided by the flux of phosphorylation of ADP to ATP (Eq. 1). These are not fixed stoichiometries due to ion leaks and proton slip. (B) Phosphorylation-pathway catalyzed by the proton pump F<sub>1</sub>F<sub>0</sub>-ATPase (F-ATPase), adenine nucleotide translocase, and inorganic phosphate transporter. The  $H^+_{neg}/P$  stoichiometry is the sum of the coupling stoichiometry in the F-ATPase reaction ( $-2.7 H^+_{pos}$  from the positive intermembrane space,  $2.7 H^+_{neg}$  to the matrix, i.e., the negative compartment) and the proton balance in the translocation of ADP<sup>2-</sup>, ATP<sup>3-</sup> and P<sub>i</sub><sup>2-</sup>. Modified from (A) Lemieux *et al.* (2017) and (B) Gnaiger (2014).

4. Mitochondrial coupling states are defined according to the control of respiratory oxygen consumption by the protonmotive force. Capacities of oxidative phosphorylation and electron transfer capacities are measured at kinetically saturating concentrations of fuel substrates, ADP and inorganic phosphate, or at optimal uncoupler concentrations, respectively. Respiratory capacities are a measure of the upper bound of the rates of respiration, providing reference values for the diagnosis of health and disease, and for evaluation of the effects of Evolutionary background, Age, Gender and sex, Lifestyle and Environment (EAGLE).
5. Some degree of uncoupling is a characteristic of energy-transformations across membranes. Uncoupling is caused by a variety of physiological, pathological, toxicological, pharmacological and environmental conditions that exert an influence not only on the proton leak and cation cycling, but also on proton slip within the proton pumps and the structural integrity of the mitochondria. A more loosely coupled state is induced by stimulation of mitochondrial superoxide formation and the bypass of proton pumps. In addition, uncoupling by application of protonophores represents an experimental intervention for the transition from a well-coupled to the noncoupled state of mitochondrial respiration.
6. Respiratory oxygen consumption rates have to be carefully normalized to enable meta-analytic studies beyond the specific question of a particular experiment. Therefore, all raw data should be published in a supplemental table or open access data repository. Normalization of rates for the volume of the experimental chamber (the measuring system) is distinguished from normalization for (1) the volume or mass of the experimental sample, (2) the number of objects (cells, organisms), and (3) the concentration of mitochondrial markers in the chamber.
7. The consistent use of terms and symbols discussed in this MitoEAGLE position statement will facilitate transdisciplinary communication and support further developments of a database on bioenergetics and mitochondrial physiology. The present considerations are focused on studies with mitochondrial preparations. These will be extended in a series of reports on pathway control of mitochondrial respiration, the protonmotive force, respiratory states in intact cells, and harmonization of experimental procedures.

---

### Box 1: In brief – Mitochondria and Bioblasts

**Mitochondria** are the oxygen-consuming electrochemical generators evolved from endosymbiotic bacteria (Margulis 1970; Lane 2005). They were described by Richard Altmann (1894) as ‘bioblasts’, which include not only the mitochondria as presently defined, but also symbiotic and free-living bacteria. The word ‘mitochondria’ (Greek mitos: thread; chondros: granule) was introduced by Carl Benda (1898).

Mitochondrial dysfunction is associated with a wide variety of genetic and degenerative diseases. Robust mitochondrial function is supported by physical exercise and caloric balance, and is central for sustained metabolic health throughout life. Therefore, a more consistent presentation of mitochondrial physiology will improve our understanding of the etiology of disease, the diagnostic repertoire of mitochondrial medicine, with a focus on protective medicine, lifestyle and healthy aging.

We now recognize mitochondria as dynamic organelles with a double membrane that are contained within eukaryotic cells. The mitochondrial inner membrane (mtIM) shows dynamic tubular to disk-shaped cristae that separate the mitochondrial matrix, *i.e.*, the negatively charged



internal mitochondrial compartment, and the intermembrane space; the latter being positively charged and enclosed by the mitochondrial outer membrane (mtOM). The mtIM contains the non-bilayer phospholipid cardiolipin, which is not present in any other eukaryotic cellular membrane. Cardiolipin promotes the formation of respiratory supercomplexes, which are supramolecular assemblies based upon specific, though dynamic, interactions between individual respiratory complexes (Greggio *et al.* 2017; Lenaz *et al.* 2017). Membrane fluidity exerts an influence on functional properties of proteins incorporated in the membranes (Waczulikova *et al.* 2007).

Mitochondria are the structural and functional elements of cell respiration. Cell respiration is the consumption of oxygen by electron transfer coupled to electrochemical proton translocation across the mtIM. In the process of oxidative phosphorylation (OXPHOS), the reduction of O<sub>2</sub> is electrochemically coupled to the transformation of energy in the form of adenosine triphosphate (ATP; Mitchell 1961, 2011). Mitochondria are the powerhouses of the cell which contain the machinery of the OXPHOS-pathways, including transmembrane respiratory complexes—proton pumps with FMN, Fe-S and cytochrome *b*, *c*, *aa*<sub>3</sub> redox systems); alternative dehydrogenases and oxidases; the coenzyme ubiquinone (Q); F-ATPase or ATP synthase; the enzymes of the tricarboxylic acid cycle and fatty acid oxidation; transporters of ions, metabolites and co-factors; and mitochondrial kinases related to energy transfer pathways. The mitochondrial proteome comprises over 1,200 proteins (Calvo *et al.* 2015; 2017), mostly encoded by nuclear DNA (nDNA), with a variety of functions, many of which are relatively well known (*e.g.*, apoptosis-regulating proteins), while others are still under investigation, or need to be identified (*e.g.*, alanine transporter).

There is a constant crosstalk between mitochondria and the other cellular components. The crosstalk between mitochondria and endoplasmic reticulum is involved in the regulation of calcium homeostasis, cell division, autophagy, differentiation, anti-viral signaling (Murley and Nunnari 2016). Cellular mitostasis is maintained through regulation at both the transcriptional and post-translational level, through cell signalling including proteostatic (*e.g.*, the ubiquitin-proteasome and autophagy-lysosome pathways), and genome stability modules throughout the cell cycle or even cell death, contributing to homeostatic regulation in response to varying energy demands and stress (Quiros *et al.* 2016). In addition to mitochondrial movement along the microtubules, mitochondrial morphology can change in response to energy requirements of the cell via processes known as fusion and fission, through which mitochondria communicate within a network, and in response to intracellular stress factors causing swelling and ultimately permeability transition.

Mitochondria typically maintain several copies of their own genome known as mitochondrial DNA (mtDNA; hundred to thousands per cell; Cummins 1998), which is maternally inherited. One exception to strictly maternal inheritance in animals is found in bivalves (Breton *et al.* 2007; White *et al.* 2008). mtDNA is 16.5 kB in length, contains 13 protein-coding genes for subunits of the transmembrane respiratory Complexes CI, CIII, CIV and F-ATPase, and also encodes 22 tRNAs and the mitochondrial 16S and 12S rRNA. Additional gene content is encoded in the mitochondrial genome, *e.g.*, microRNAs, piRNA, smithRNAs, repeat associated RNA, and even additional proteins (Duarte *et al.* 2014; Lee *et al.* 2015; Cobb *et al.* 2016). The mitochondrial genome is regulated and supplemented by nuclear-encoded mitochondrial targeted proteins.

Abbreviation: mt, as generally used in mtDNA. Mitochondrion is singular and mitochondria is plural.

*‘For the physiologist, mitochondria afforded the first opportunity for an experimental approach to structure-function relationships, in particular those involved in active transport, vectorial metabolism, and metabolic control mechanisms on a subcellular level’* (Ernster and Schatz 1981).

## 1. Introduction

Mitochondria are the powerhouses of the cell with numerous physiological, molecular, and genetic functions (**Box 1**). Every study of mitochondrial health and disease is faced with Evolution, Age, Gender and sex, Lifestyle, and Environment (EAGLE) as essential background conditions intrinsic to the individual patient or subject, cohort, species, tissue and to some extent even cell line. As a large and coordinated group of laboratories and researchers, the mission of the global MitoEAGLE Network is to generate the necessary scale, type, and quality of consistent data sets and conditions to address this intrinsic complexity. Harmonization of experimental protocols and implementation of a quality control and data management system are required to interrelate results gathered across a spectrum of studies and to generate a rigorously monitored database focused on mitochondrial respiratory function. In this way, researchers within the same and across different disciplines will be positioned to compare findings across traditions and generations to an agreed upon set of clearly defined and accepted international standards.

Reliability and comparability of quantitative results depend on the accuracy of measurements under strictly-defined conditions. A conceptual framework is required to warrant meaningful interpretation and comparability of experimental outcomes carried out by research groups at different institutes. With an emphasis on quality of research, collected data can be useful far beyond the specific question of a particular experiment. Enabling meta-analytic studies is the most economic way of providing robust answers to biological questions (Cooper *et al.* 2009). Vague or ambiguous jargon can lead to confusion and may relegate valuable signals to wasteful noise. For this reason, measured values must be expressed in standard units for each parameter used to define mitochondrial respiratory function. Harmonization of nomenclature and definition of technical terms are essential to improve the awareness of the intricate meaning of current and past scientific vocabulary, for documentation and integration into databases in general, and quantitative modelling in particular (Beard 2005). The focus on coupling states and fluxes through metabolic pathways of aerobic energy transformation in mitochondrial preparations is a first step in the attempt to generate a conceptually-oriented nomenclature in bioenergetics and mitochondrial physiology. Coupling states of intact cells, the protonmotive force, and respiratory control by fuel substrates and specific inhibitors of respiratory enzymes will be reviewed in subsequent communications.

## 2. Oxidative phosphorylation and coupling states in mitochondrial preparations

*‘Every professional group develops its own technical jargon for talking about matters of critical concern ... People who know a word can share that idea with other members of their group, and a shared vocabulary is part of the glue that holds people together and allows them to create a shared culture’ (Miller 1991).*

**Mitochondrial preparations** are defined as either isolated mitochondria, or tissue and cellular preparations in which the barrier function of the plasma membrane is disrupted. Since this entails the loss of cell viability, mitochondrial preparations are not studied *in vivo*. In contrast to isolated mitochondria and tissue homogenate preparations, mitochondria in permeabilized tissues and cells are *in situ* relative to the plasma membrane. The plasma membrane separates the intracellular compartment including the cytosol, nucleus, and organelles from the environment of the cell. The plasma membrane consists of a lipid bilayer, embedded proteins, and attached organic molecules that collectively control the selective permeability of ions, organic molecules, and particles across the cell boundary. The intact plasma membrane prevents the passage of many water-soluble mitochondrial substrates and inorganic ions—such as succinate, adenosine diphosphate (ADP) and inorganic phosphate (P<sub>i</sub>),

that must be controlled at kinetically-saturating concentrations for the analysis of respiratory capacities; this limits the scope of investigations into mitochondrial respiratory function in intact cells.

The cholesterol content of the plasma membrane is high compared to mitochondrial membranes. Therefore, mild detergents—such as digitonin and saponin—can be applied to selectively permeabilize the plasma membrane by interaction with cholesterol and allow free exchange of organic molecules and inorganic ions between the cytosol and the immediate cell environment, while maintaining the integrity and localization of organelles, cytoskeleton, and the nucleus. Application of optimum concentrations of permeabilization agents (mild detergents or toxins) leads to the complete loss of cell viability, tested by nuclear staining and washout of cytosolic marker enzymes—such as lactate dehydrogenase, while mitochondrial function remains intact. The respiration rate of isolated mitochondria remains unaltered after the addition of low concentrations of digitonin or saponin. In addition to mechanical permeabilization during homogenization of tissue, permeabilization agents may be applied to ensure permeabilization of all cells. Suspensions of cells permeabilized in the respiration chamber and crude tissue homogenates contain all components of the cell at highly dilute concentrations. All mitochondria are retained in chemically-permeabilized mitochondrial preparations and crude tissue homogenates. In the preparation of isolated mitochondria, the cells or tissues are homogenized, and the mitochondria are separated from other cell fractions and purified by differential centrifugation, entailing the loss of a fraction of mitochondria. Typical mitochondrial recovery ranges from 30% to 80%. Maximization of the purity of isolated mitochondria may compromise not only the mitochondrial yield but also the structural and functional integrity. Therefore, protocols to isolate mitochondria need to be optimized according to each study. The term mitochondrial preparation does not include further fractionation of mitochondrial components, neither submitochondrial particles.

### 2.1. Respiratory control and coupling

Respiratory coupling control states are established in studies of mitochondrial preparations to obtain reference values for various output variables. Physiological conditions *in vivo* deviate from these experimentally obtained states. Since kinetically-saturating concentrations, *e.g.*, of ADP or oxygen, may not apply to physiological intracellular conditions, relevant information is obtained in studies of kinetic responses to variations in [ADP] or [O<sub>2</sub>] in the range between kinetically-saturating concentrations and anoxia (Gnaiger 2001).

**The steady-state:** Mitochondria represent a thermodynamically open system in non-equilibrium states of biochemical energy transformation. State variables (protonmotive force; redox states) and metabolic *rates* (fluxes) are measured in defined mitochondrial respiratory states. Steady-states can be obtained only in open systems, in which changes by *internal* transformations, *e.g.*, O<sub>2</sub> consumption, are instantaneously compensated for by *external* fluxes, *e.g.*, O<sub>2</sub> supply, preventing a change of oxygen concentration in the system (Gnaiger 1993b). Mitochondrial respiratory states monitored in closed systems satisfy the criteria of pseudo-steady states for limited periods of time, when changes in the system (concentrations of O<sub>2</sub>, fuel substrates, ADP, P<sub>i</sub>, H<sup>+</sup>) do not exert significant effects on metabolic fluxes (respiration, phosphorylation). Such pseudo-steady states require respiratory media with sufficient buffering capacity and substrates maintained at kinetically-saturating concentrations, and thus depend on the kinetics of the processes under investigation.

**Specification of biochemical dose:** Substrates, uncouplers, inhibitors, and other biochemical reagents are titrated to dissect mitochondrial function. Nominal concentrations of these substances are usually reported as initial amount of substance concentration [mol·L<sup>-1</sup>] in the incubation medium. When aiming at the measurement of kinetically saturated processes—such as OXPHOS-capacities, the concentrations for substrates can be chosen according to the



apparent equilibrium constant,  $K_m'$ . In the case of hyperbolic kinetics, only 80% of maximum respiratory capacity is obtained at a substrate concentration of four times the  $K_m'$ , whereas substrate concentrations of 5, 9, 19 and 49 times the  $K_m'$  are theoretically required for reaching 83%, 90%, 95% or 98% of the maximal rate (Gnaiger 2001). Other reagents are chosen to inhibit or alter some process. The amount of these chemicals in an experimental incubation is selected to maximize effect, yet not lead to unacceptable off-target consequences that would adversely affect the data being sought. Specifying the amount of substance in an incubation as nominal concentration in the aqueous incubation medium can be ambiguous (Doskey *et al.* 2015), particularly when lipophilic substances (oligomycin uncouplers, permeabilization agents) or cations ( $\text{TPP}^+$ ; fluorescent dyes such as safranin, TMRM) are applied which accumulate in biological membranes or the mitochondrial matrix. For example, a dose of digitonin of  $8 \text{ fmol} \cdot \text{cell}^{-1}$  ( $10 \text{ pg} \cdot \text{cell}^{-1}$ ;  $10 \text{ } \mu\text{g} \cdot 10^{-6} \text{ cells}$ ) is optimal for permeabilization of endothelial cells, and the concentration in the incubation medium has to be adjusted according to the cell density applied (Doerrier *et al.* 2018). Generally, dose/exposure can be specified per unit of biological sample, *i.e.*, (nominal moles of xenobiotic)/(number of cells) [ $\text{mol} \cdot \text{cell}^{-1}$ ] or, as appropriate, per mass of biological sample [ $\text{mol} \cdot \text{kg}^{-1}$ ]. This approach to specification of dose/exposure provides a scalable parameter that can be used to design experiments, help interpret a wide variety of experimental results, and provide absolute information that allows researchers worldwide to make the most use of published data (Doskey *et al.* 2015).

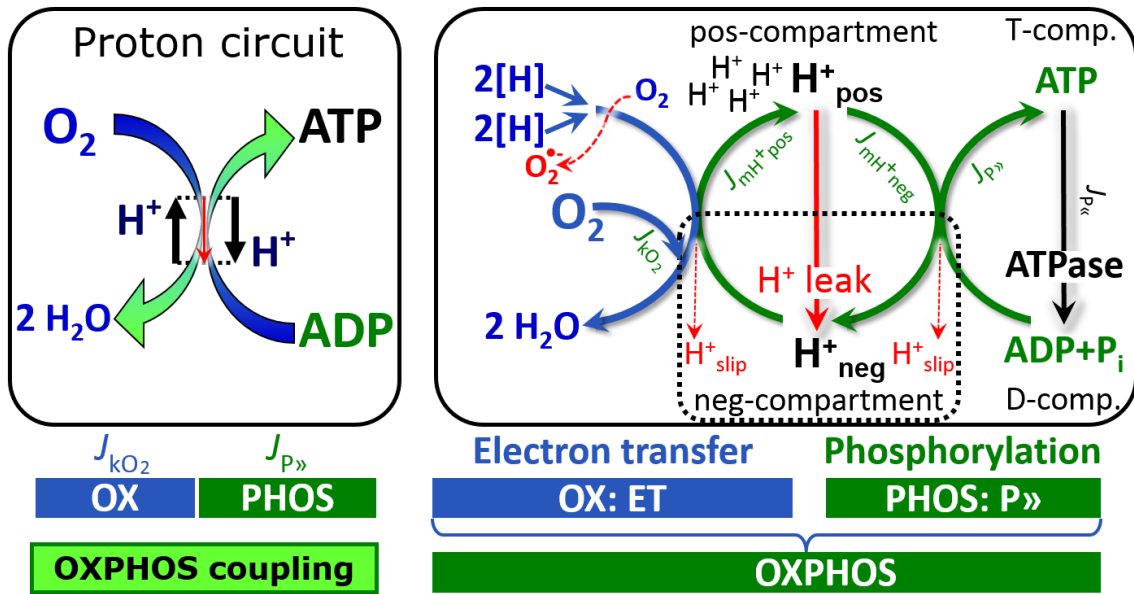


**Fig. 2. The proton circuit and coupling in oxidative phosphorylation (OXPHOS).** 2[H] indicates the reduced hydrogen equivalents of fuel substrates of the catabolic reaction  $k$  with oxygen. Oxygen flux,  $J_{kO_2}$ , through the catabolic ET-pathway, is coupled to flux through the phosphorylation-pathway of ADP to ATP,  $J_{P\gg}$ . The proton pumps of the ET-pathway drive proton flux into the positive (pos) compartment,  $J_{mH^+pos}$ , generating the output protonmotive force (motive, subscript  $m$ ). F-ATPase is coupled to inward proton current into the negative (neg) compartment,  $J_{mH^+neg}$ , to phosphorylate  $\text{ADP} + \text{P}_i$  to ATP. The system defined by the boundaries (full black line) is not a black box, but is analysed as a compartmental system. The negative compartment (neg-compartment, enclosed by the dotted line) is the matrix space, separated by the mtIM from the positive compartment (pos-compartment).  $\text{ADP} + \text{P}_i$  and ATP are the substrate- and product-compartments (scalar ADP and ATP compartments, D-comp. and T-comp.), respectively. At steady-state proton turnover,  $J_{\infty H^+}$ , and ATP turnover,  $J_{P\infty}$ , maintain concentrations constant, when  $J_{mH^+\infty} = J_{mH^+pos} = J_{mH^+neg}$ , and  $J_{P\infty} = J_{P\gg} = J_{P\ll}$ . Modified from Gnaiger (2014).

**Phosphorylation, P», and P»/O<sub>2</sub> ratio:** *Phosphorylation* in the context of OXPHOS is defined as phosphorylation of **ADP by P<sub>i</sub> to ATP**. On the other hand, the term phosphorylation is used generally in many contexts, *e.g.*, protein phosphorylation. This justifies consideration of a symbol more discriminating and specific than P as used in the P/O ratio (phosphate to atomic oxygen ratio), where P indicates phosphorylation of ADP to ATP or GDP to GTP. We propose the symbol P» for the endergonic (uphill) direction of phosphorylation ADP→ATP, and likewise the symbol P« for the corresponding exergonic (downhill) hydrolysis ATP→ADP (**Fig. 2**). P» refers mainly to electrontransfer phosphorylation but may also involve substrate-level phosphorylation as part of the tricarboxylic acid (TCA) cycle (succinyl-CoA ligase) and phosphorylation of ADP catalyzed by phosphoenolpyruvate carboxykinase. Transphosphorylation is performed by adenylate kinase, creatine kinase, hexokinase and nucleoside diphosphate kinase. In isolated mammalian mitochondria, ATP production catalyzed by adenylate kinase (2 ADP ↔ ATP + AMP) proceeds without fuel substrates in the presence of ADP (Komlódi and Tretter 2017). Kinase cycles are involved in intracellular energy transfer and signal transduction for regulation of energy flux.

The P»/O<sub>2</sub> ratio (P»/4 e<sup>-</sup>) is two times the ‘P/O’ ratio (P»/2 e<sup>-</sup>) of classical bioenergetics. P»/O<sub>2</sub> is a generalized symbol, independent phosphorylation assessment by determination of P<sub>i</sub> consumption (P<sub>i</sub>/O<sub>2</sub> flux ratio), ADP depletion (ADP/O<sub>2</sub> flux ratio), or ATP production (ATP/O<sub>2</sub> flux ratio). The mechanistic P»/O<sub>2</sub> ratio—or P»/O<sub>2</sub> stoichiometry—is calculated from the proton-to-oxygen and proton-to-phosphorylation coupling stoichiometries (**Fig. 1A**),

$$P»/O_2 = \frac{H_{pos}^+/O_2}{H_{neg}^+/P»} \quad (1)$$

The H<sub>pos</sub><sup>+</sup>/O<sub>2</sub> *coupling stoichiometry* (referring to the full 4 electron reduction of O<sub>2</sub>) depends on the ET-pathway control state which defines the relative involvement of the three coupling sites (CI, CIII and CIV) in the catabolic pathway of electrons to O<sub>2</sub>. This varies with: (1) a bypass of CI by single or multiple electron input into the Q-junction; and (2) a bypass of CIV by involvement of AOX. H<sub>pos</sub><sup>+</sup>/O<sub>2</sub> is 12 in the ET-pathways involving CIII and CIV as proton pumps, increasing to 20 for the NADH-pathway (**Fig. 1A**), but a general consensus on H<sub>pos</sub><sup>+</sup>/O<sub>2</sub> stoichiometries remains to be reached (Hinkle 2005; Wikström and Hummer 2012; Sazanov 2015). The H<sub>neg</sub><sup>+</sup>/P» coupling stoichiometry (3.7; **Fig. 1A**) is the sum of 2.7 H<sub>neg</sub><sup>+</sup> required by the F-ATPase of vertebrate and most invertebrate species (Watt *et al.* 2010) and the proton balance in the translocation of ADP, ATP and P<sub>i</sub> (**Fig. 1B**). Taken together, the mechanistic P»/O<sub>2</sub> ratio is calculated at 5.4 and 3.3 for NADH- and succinate-linked respiration, respectively (Eq. 1). The corresponding classical P»/O ratios (referring to the 2 electron reduction of 0.5 O<sub>2</sub>) are 2.7 and 1.6 (Watt *et al.* 2010), in agreement with the measured P»/O ratio for succinate of 1.58 ± 0.02 (Gnaiger *et al.* 2000).

The effective P»/O<sub>2</sub> flux ratio (Y<sub>P»/O<sub>2</sub></sub> = J<sub>P»</sub>/J<sub>kO<sub>2</sub></sub>) is diminished relative to the mechanistic P»/O<sub>2</sub> ratio by intrinsic and extrinsic uncoupling and dyscoupling (**Fig. 3**). Such generalized uncoupling is different from switching to mitochondrial pathways that involve fewer than three proton pumps (‘coupling sites’: Complexes CI, CIII and CIV), bypassing CI through multiple electron entries into the Q-junction, or CIII and CIV through AOX (**Fig. 1**). Reprogramming of mitochondrial pathways may be considered as a switch of gears (changing the stoichiometry) rather than uncoupling (loosening the stoichiometry). In addition, Y<sub>P»/O<sub>2</sub></sub> depends on several experimental conditions of flux control, increasing as a hyperbolic function of [ADP] to a maximum value (Gnaiger 2001).

**Control and regulation:** The terms metabolic *control* and *regulation* are frequently used synonymously, but are distinguished in metabolic control analysis: ‘We could understand the regulation as the mechanism that occurs when a system maintains some variable constant over time, in spite of fluctuations in external conditions (homeostasis of the internal state). On the

other hand, metabolic control is the power to change the state of the metabolism in response to an external signal' (Fell 1997). Respiratory control may be induced by experimental control signals that *exert* an influence on: (1) ATP demand and ADP phosphorylation-rate; (2) fuel substrate composition, pathway competition; (3) available amounts of substrates and oxygen, *e.g.*, starvation and hypoxia; (4) the protonmotive force, redox states, flux–force relationships, coupling and efficiency; (5)  $\text{Ca}^{2+}$  and other ions including  $\text{H}^+$ ; (6) inhibitors, *e.g.*, nitric oxide or intermediary metabolites such as oxaloacetate; (7) signalling pathways and regulatory proteins, *e.g.*, insulin resistance, transcription factor hypoxia inducible factor 1. *Mechanisms* of respiratory control and regulation include adjustments of: (1) enzyme activities by allosteric mechanisms and phosphorylation; (2) enzyme content, concentrations of cofactors and conserved moieties—such as adenylates, nicotinamide adenine dinucleotide [ $\text{NAD}^+/\text{NADH}$ ], coenzyme Q, cytochrome *c*); (3) metabolic channeling by supercomplexes; and (4) mitochondrial density (enzyme concentrations and membrane area) and morphology (cristae folding, fission and fusion). Mitochondria are targeted directly by hormones, thereby affecting their energy metabolism (Lee *et al.* 2013; Gerö and Szabo 2016; Price and Dai 2016; Moreno *et al.* 2017). Evolutionary or acquired differences in the genetic and epigenetic basis of mitochondrial function (or dysfunction) between subjects and gene therapy; age; gender, biological sex, and hormone concentrations; life style including exercise and nutrition; and environmental issues including thermal, atmospheric, toxicological and pharmacological factors, exert an influence on all control mechanisms listed above. For reviews, see Brown 1992; Gnaiger 1993a, 2009; 2014; Paradies *et al.* 2014; Morrow *et al.* 2017.

**Respiratory control and response:** Lack of control by a metabolic pathway, *e.g.*, phosphorylation-pathway, means that there will be no response to a variable activating it, *e.g.*, [ADP]. The reverse, however, is not true as the absence of a response to [ADP] does not exclude the phosphorylation-pathway from having some degree of control. The degree of control of a component of the OXPHOS-pathway on an output variable—such as oxygen flux, will in general be different from the degree of control on other outputs—such as phosphorylation-flux or proton leak flux. Therefore, it is necessary to be specific as to which input and output are under consideration (Fell 1997).

**Respiratory coupling control and ET-pathway control:** Respiratory control refers to the ability of mitochondria to adjust oxygen consumption in response to external control signals by engaging various mechanisms of control and regulation. Respiratory control is monitored in a mitochondrial preparation under conditions defined as respiratory states. When phosphorylation of ADP to ATP is stimulated or depressed, an increase or decrease is observed in electron flux linked to oxygen consumption in respiratory coupling states of intact mitochondria ('controlled states' in the classical terminology of bioenergetics). Alternatively, coupling of electron transfer with phosphorylation is disengaged by disruption of the integrity of the mtIM or by uncouplers, functioning like a clutch in a mechanical system. The corresponding coupling control state is characterized by high levels of oxygen consumption without control by  $\text{P}_i$  ('uncontrolled state').

ET-pathway control states are obtained in mitochondrial preparations by depletion of endogenous substrates and addition to the mitochondrial respiration medium of fuel substrates ( $\text{CHNO}$ ;  $2[\text{H}]$  in Fig. 2) and specific inhibitors, activating selected mitochondrial catabolic pathways,  $\text{K}^+$  (Fig. 1). Coupling control states and pathway control states are complementary, since mitochondrial preparations depend on an exogenous supply of pathway-specific fuel substrates and oxygen (Gnaiger 2014).

**Coupling:** In mitochondrial electron transfer (Fig. 1), vectorial transmembrane proton flux is coupled through the proton pumps CI, CIII and CIV to the catabolic flux of scalar reactions, collectively measured as oxygen flux (Fig. 2). Thus mitochondria are elements of energy transformation. Energy cannot be lost or produced in any internal process (First Law of thermodynamics). Open and closed systems can gain or loose energy only by external fluxes—

by exchange with the environment. Energy is a conserved quantity. Therefore, energy can neither be produced by mitochondria, nor is there any internal process without energy conservation. Exergy is defined as the 'free energy' with the potential to perform work. *Coupling* is the mechanistic linkage of an exergonic process (spontaneous, negative exergy change) with an endergonic process (positive exergy change) in energy transformations which conserve part of the exergy that would be irreversibly lost or dissipated in an uncoupled process.

**Uncoupling:** Uncoupling of mitochondrial respiration is a general term comprising diverse mechanisms. Differences of terms—uncoupled *vs.* noncoupled—are easily overlooked, although they relate to different mechanisms of uncoupling (Fig. 3).

1. Proton leak across the mtIM from the pos- to the neg-compartment (Fig. 2);
2. Cycling of other cations, strongly stimulated by permeability transition;
3. Proton slip in the proton pumps when protons are effectively not pumped (CI, CIII and CIV) or are not driving phosphorylation (F-ATPase);
4. Loss of compartmental integrity when electron transfer is uncoupled;
5. Electron leak in the loosely coupled univalent reduction of oxygen ( $O_2$ ; dioxygen) to superoxide ( $O_2^{\bullet -}$ ; superoxide anion radical).

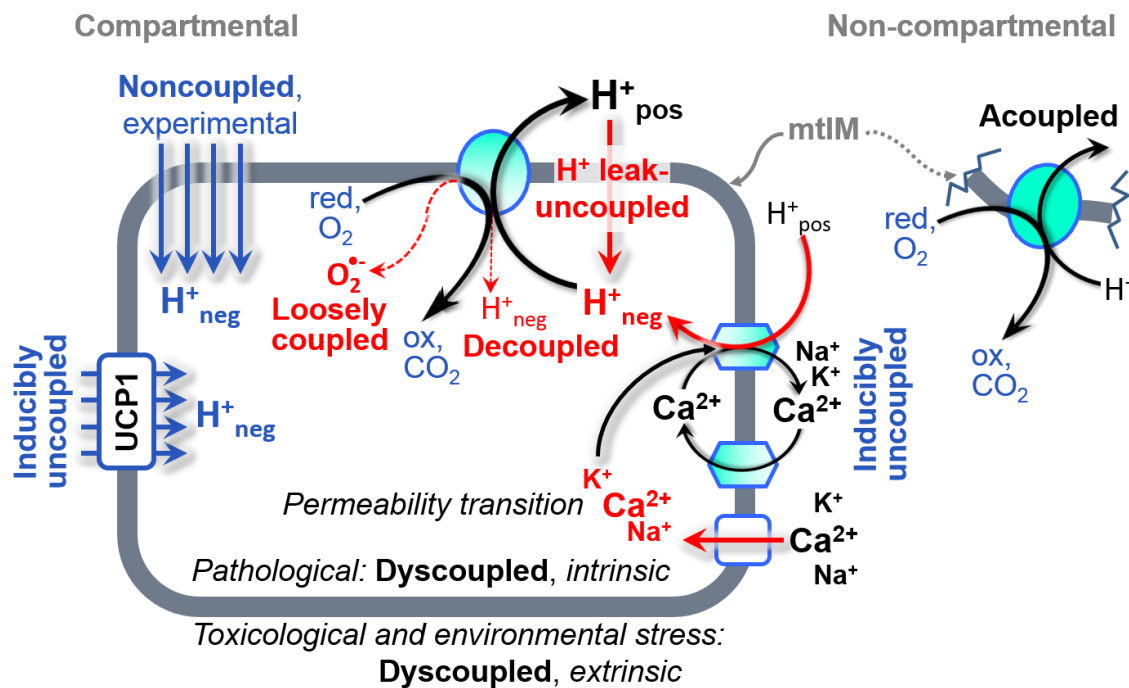


**Fig 3. Mechanisms of respiratory uncoupling.** An intact mitochondrial inner membrane, mtIM, is required for vectorial, compartmental coupling. 'Acoupled' respiration is the consequence of structural disruption with catalytic activity of non-compartmental mitochondrial fragments. Inducibly uncoupled (activation of UCP1) and experimentally noncoupled respiration (titration of protonophores) stimulate respiration to maximum oxygen flux.  $H^+$  leak-uncoupled, decoupled, and loosely coupled respiration are components of intrinsic uncoupling. Pathological dysfunction may affect all types of uncoupling, including permeability transition, causing intrinsically dyscoupled respiration. Similarly, toxicological and environmental stress factors can cause extrinsically dyscoupled respiration.

## 2.2. Coupling states and respiratory rates

**Respiratory capacities in coupling control states:** To extend the classical nomenclature on mitochondrial coupling states (Section 2.3) by a concept-driven terminology that incorporates explicitly information on the nature of respiratory states, the terminology must be



general and not restricted to any particular experimental protocol or mitochondrial preparation (Gnaiger 2009). We focus primarily on the conceptual ‘why’, along with clarification of the experimental ‘how’. Respiratory capacities delineate, comparable to channel capacity in information theory (Schneider 2006), the upper bound of the rate of respiration measured in defined coupling control states and electron transfer-pathway (ET-pathway) states (Fig. 4).

**Fig. 4. Four-compartment model of oxidative phosphorylation.**

Respiratory states (ET, OXPHOS, LEAK; Table 1) and corresponding rates ( $E$ ,  $P$ ,  $L$ ) are connected by the protonmotive force,  $\Delta p$ . ET-capacity,  $E$ , is partitioned into (1) dissipative LEAK-respiration,  $L$ , when the Gibbs energy change of catabolic  $O_2$  consumption is

irreversibly lost, (2) net OXPHOS-capacity,  $P-L$ , with partial conservation of the capacity to perform work, and (3) the excess capacity,  $E-P$ . Modified from Gnaiger (2014).

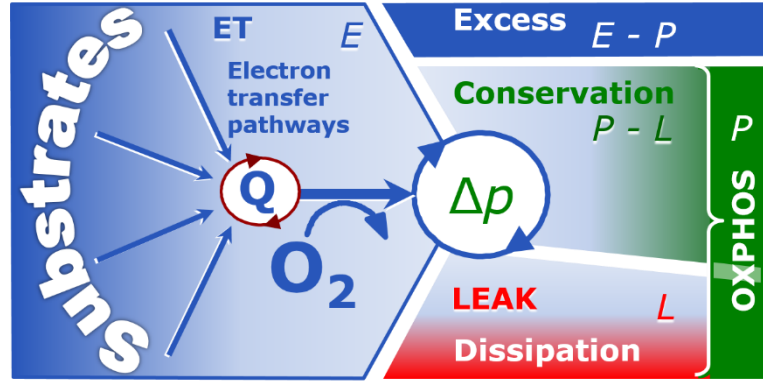


**Table 1. Coupling states and residual oxygen consumption in mitochondrial preparations in relation to respiration- and phosphorylation-rate,  $J_{kO_2}$  and  $J_{P_{\gg}}$ , and protonmotive force,  $\Delta p$ .** Coupling states are established at kinetically-saturating concentrations of fuel substrates and  $O_2$ .

State	$J_{kO_2}$	$J_{P_{\gg}}$	$\Delta p$	Inducing factors	Limiting factors
LEAK	$L$ ; low, cation leak-dependent respiration	0	max.	proton leak, slip, and cation cycling	$J_{P_{\gg}} = 0$ : (1) without ADP, $L_N$ ; (2) max. ATP/ADP ratio, $L_T$ ; or (3) inhibition of the phosphorylation-pathway, $L_{Omy}$
OXPHOS	$P$ ; high, ADP-stimulated respiration	max.	high	kinetically-saturating [ADP] and $[P_i]$	$J_{P_{\gg}}$ by phosphorylation-pathway; or $J_{kO_2}$ by ET-capacity
ET	$E$ ; max., noncoupled respiration	0	low	optimal external uncoupler concentration for max. $J_{O_2, E}$	$J_{kO_2}$ by ET-capacity
ROX	$R_{ox}$ ; min., residual $O_2$ consumption	0	0	$J_{O_2, Rox}$ in non-ET-pathway oxidation reactions	full inhibition of ET-pathway; or absence of fuel substrates

To provide a diagnostic reference for respiratory capacities of core energy metabolism, the capacity of *oxidative phosphorylation*, OXPHOS, is measured at kinetically-saturating concentrations of ADP and  $P_i$ . The *oxidative* ET-capacity reveals the limitation of OXPHOS-capacity mediated by the *phosphorylation*-pathway. The ET- and phosphorylation-pathways comprise coupled segments of the OXPHOS-system. ET-capacity is measured as noncoupled respiration by application of *external uncouplers*. The contribution of *intrinsically uncoupled*



oxygen consumption is studied in the absence of ADP—by not stimulating phosphorylation, or by inhibition of the phosphorylation-pathway. The corresponding states are collectively classified as LEAK-states, when oxygen consumption compensates mainly for ion leaks, including the proton leak. Defined coupling states are induced by: (1) adding cation chelators such as EGTA, binding free  $\text{Ca}^{2+}$  and thus limiting cation cycling; (2) adding ADP and  $\text{P}_i$ ; (3) inhibiting the phosphorylation-pathway; and (4) uncoupler titrations, while maintaining a defined ET-pathway state with constant fuel substrates and inhibitors of specific branches of the ET-pathway (Fig. 1).

The three coupling states, ET, LEAK and OXPHOS, are shown schematically with the corresponding respiratory rates, abbreviated as  $E$ ,  $L$  and  $P$ , respectively (Fig. 4). We distinguish metabolic *pathways* from metabolic *states* and the corresponding metabolic *rates*; for example: ET-pathways (Fig. 4), ET-state (Fig. 5C), and ET-capacity,  $E$ , respectively (Table 1). The protonmotive force is *high* in the OXPHOS-state when it drives phosphorylation, *maximum* in the LEAK-state of coupled mitochondria, driven by LEAK-respiration at a minimum back flux of cations to the matrix side, and *very low* in the ET-state when uncouplers short-circuit the proton cycle (Table 1).

$E$  may exceed or be equal to  $P$ .  $E > P$  is observed in many types of mitochondria, varying between species, tissues and cell types (Gnaiger 2009).  $E - P$  is the excess ET-capacity pushing the phosphorylation-flux (Fig. 1B) to the limit of its *capacity of utilizing* the protonmotive force. In addition, the magnitude of  $E - P$  depends on the tightness of respiratory coupling or degree of uncoupling, since an increase of  $L$  causes  $P$  to increase towards the limit of  $E$ . The *excess*  $E - P$  capacity,  $E - P$ , therefore, provides a sensitive diagnostic indicator of specific injuries of the phosphorylation-pathway, under conditions when  $E$  remains constant but  $P$  declines relative to controls (Fig. 4). Substrate cocktails supporting simultaneous convergent electron transfer to the Q-junction for reconstitution of TCA cycle function establish pathway control states with high ET-capacity, and consequently increase the sensitivity of the  $E - P$  assay.

$E$  cannot theoretically be lower than  $P$ .  $E < P$  must be discounted as an artefact, which may be caused experimentally by: (1) loss of oxidative capacity during the time course of the respirometric assay, since  $E$  is measured subsequently to  $P$ ; (2) using insufficient uncoupler concentrations; (3) using high uncoupler concentrations which inhibit ET (Gnaiger 2008); (4) high oligomycin concentrations applied for measurement of  $L$  before titrations of uncoupler, when oligomycin exerts an inhibitory effect on  $E$ . On the other hand, the excess ET-capacity is overestimated if non-saturating  $[\text{ADP}]$  or  $[\text{P}_i]$  are used. See State 3 in the next section.

The net OXPHOS-capacity is calculated by subtracting  $L$  from  $P$  (Fig. 4). Then the net  $P \gg \text{O}_2$  equals  $P \gg (P - L)$ , wherein the dissipative LEAK component in the OXPHOS-state may be overestimated. This can be avoided by measuring LEAK-respiration in a state when the protonmotive force is adjusted to its slightly lower value in the OXPHOS-state—by titration of an ET inhibitor (Divakaruni and Brand 2011). Any turnover-dependent components of proton leak and slip, however, are underestimated under these conditions (Garlid *et al.* 1993). In general, it is inappropriate to use the term *ATP production* or *ATP turnover* for the difference of oxygen consumption measured in states  $P$  and  $L$ . The difference  $P - L$  is the upper limit of the part of OXPHOS-capacity that is freely available for ATP production (corrected for LEAK-respiration) and is fully coupled to phosphorylation with a maximum mechanistic stoichiometry (Fig. 4).

**LEAK-state (Fig. 5A):** The LEAK-state is defined as a state of mitochondrial respiration when  $\text{O}_2$  flux mainly compensates for ion leaks in the absence of ATP synthesis, at kinetically-saturating concentrations of  $\text{O}_2$  and respiratory fuel substrates. LEAK-respiration is measured to obtain an estimate of *intrinsic uncoupling* without addition of an experimental uncoupler: (1)

in the absence of adenylates; (2) after depletion of ADP at a maximum ATP/ADP ratio; or (3) after inhibition of the phosphorylation-pathway by inhibitors of F-ATPase—such as oligomycin, or of adenine nucleotide translocase—such as carboxyatractyloside.

Adjustment of the nominal concentration of these inhibitors to the density of biological sample applied can minimize or avoid inhibitory side-effects exerted on ET-capacity or even some dyscoupling.

**Proton leak and uncoupled respiration:** Proton leak is a leak current of protons. The intrinsic proton leak is the *uncoupled* process in which protons diffuse across the mtIM in the dissipative direction of the downhill protonmotive force without coupling to phosphorylation (Fig. 5A). The proton leak flux depends non-linearly on the protonmotive force (Garlid *et al.* 1989; Divakaruni and Brand 2011), it is a property of the mtIM and may be enhanced due to possible contaminations by free fatty acids. Inducible uncoupling mediated by uncoupling protein 1 (UCP1) is physiologically controlled, *e.g.*, in brown adipose tissue. UCP1 is a member of the mitochondrial carrier family which is involved in the translocation of protons across the mtIM (Klingenberg 2017). Consequently, the short-circuit diminishes the protonmotive force and stimulates electron transfer to O<sub>2</sub> and heat dissipation without phosphorylation of ADP.

**Cation cycling:** There can be other cation contributors to leak current including calcium and probably magnesium. Calcium current is balanced by mitochondrial Na<sup>+</sup>/Ca<sup>2+</sup> exchange, which is balanced by Na<sup>+</sup>/H<sup>+</sup> or K<sup>+</sup>/H<sup>+</sup> exchanges. This is another effective uncoupling mechanism different from proton leak.

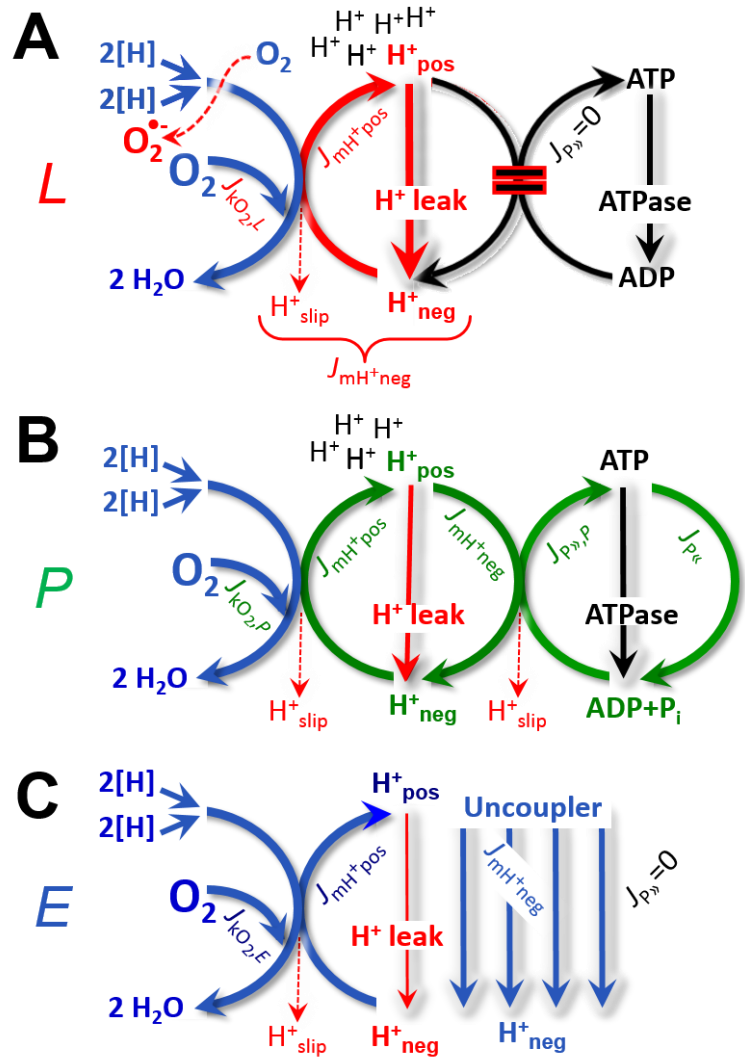


**Fig. 5. Respiratory coupling states. A: LEAK-state and rate, L:** Phosphorylation is arrested,  $J_P = 0$ , and catabolic oxygen flux,  $J_{kO_2,L}$ , is controlled mainly by the proton leak,  $J_{mH^+neg,L}$ , at maximum protonmotive force (Fig. 3). **B: OXPHOS-state and rate, P:** Phosphorylation,  $J_P$ , is stimulated by kinetically-saturating [ADP] and [P<sub>i</sub>], and is supported by a high protonmotive force. O<sub>2</sub> flux,  $J_{kO_2,P}$ , is well-coupled at a  $P \gg O_2$  ratio of  $J_{P,P}/J_{O_2,P}$ . **C: ET-state and rate, E:** Noncoupled respiration,  $J_{kO_2,E}$ , is maximum at optimum exogenous uncoupler concentration and phosphorylation is zero,  $J_P = 0$ . See also Fig. 2.

683 **Table 2. Terms on respiratory coupling and uncoupling.**

Term	$J_{\text{kO}_2}$	P»/O <sub>2</sub>	Note	
acoupled		0	electron transfer in mitochondrial fragments without vectorial proton translocation ( <b>Fig. 3</b> )	
intrinsic, no protonophore added	uncoupled	$L$	0	non-phosphorylating LEAK-respiration ( <b>Fig. 5A</b> )
	proton leak-uncoupled		0	component of $L$ , H <sup>+</sup> diffusion across the mtIM ( <b>Fig. 3</b> )
	decoupled		0	component of $L$ , proton slip ( <b>Fig. 3</b> )
	loosely coupled		0	component of $L$ , lower coupling due to superoxide formation and bypass of proton pumps ( <b>Fig. 3</b> )
	dyscoupled		0	pathologically, toxicologically, environmentally increased uncoupling, mitochondrial dysfunction
	inducibly uncoupled		0	by UCP1 or cation ( <i>e.g.</i> , Ca <sup>2+</sup> ) cycling ( <b>Fig. 3</b> )
noncoupled	$E$	0	non-phosphorylating respiration stimulated to maximum flux at optimum exogenous uncoupler concentration ( <b>Fig. 5C</b> )	
well-coupled	$P$	high	phosphorylating respiration with an intrinsic LEAK component ( <b>Fig. 5B</b> )	
fully coupled	$P - L$	max.	OXPHOS-capacity corrected for LEAK-respiration ( <b>Fig. 4</b> )	

684  
685 **Proton slip and decoupled respiration:** Proton slip is the *decoupled* process in which  
686 protons are only partially translocated by a proton pump of the ET-pathways and slip back to  
687 the original compartment. The proton leak is the dominant contributor to the overall leak current  
688 in mammalian mitochondria incubated under physiological conditions at 37 °C, whereas proton  
689 slip is increased at lower experimental temperature (Canton *et al.* 1995). Proton slip can also  
690 happen in association with the F-ATPase, in which the proton slips downhill across the pump  
691 to the matrix without contributing to ATP synthesis. In each case, proton slip is a property of  
692 the proton pump and increases with the pump turnover rate.

693 **Electron leak and loosely coupled respiration:** Superoxide production by the ETS leads  
694 to a bypass of proton pumps and correspondingly lower  $P \gg O_2$  ratio. This depends on the actual  
695 site of electron leak and the scavenging of hydrogen peroxide by cytochrome *c*, whereby  
696 electrons may re-enter the ETS with proton translocation by CIV.

697 **Loss of compartmental integrity and acoupled respiration:** Electron transfer and  $O_2$   
698 consumption proceed without compartmental proton translocation in disrupted mitochondrial  
699 fragments. Such fragments form during mitochondrial isolation, and may not fully fuse to re-  
700 establish structurally intact mitochondria. Loss of mtIM integrity, therefore, is the cause of  
701 acoupled respiration, which is a nonvectorial dissipative process without control by the  
702 protonmotive force.

703 **Dyscoupled respiration:** Mitochondrial injuries may lead to *dyscoupling* as a  
704 pathological or toxicological cause of *uncoupled* respiration. Dyscoupling may involve any  
705 type of uncoupling mechanism, *e.g.*, opening the permeability transition pore. Dyscoupled  
706 respiration is distinguished from the experimentally induced *noncoupled* respiration in the ET-  
707 state (**Fig. 3**).

708 **OXPHOS-state (Fig. 5B):** The OXPHOS-state is defined as the respiratory state with  
709 kinetically-saturating concentrations of  $O_2$ , respiratory and phosphorylation substrates, and

absence of exogenous uncoupler, which provides an estimate of the maximal respiratory capacity in the OXPHOS-state for any given ET-pathway state. Respiratory capacities at kinetically-saturating substrate concentrations provide reference values or upper limits of performance, aiming at the generation of data sets for comparative purposes. Physiological activities and effects of substrate kinetics can be evaluated relative to the OXPHOS-capacity.

As discussed previously, 0.2 mM ADP does not fully saturate flux in isolated mitochondria (Gnaiger 2001; Puchowicz *et al.* 2004); greater ADP concentration is required, particularly in permeabilized muscle fibres and cardiomyocytes, to overcome limitations by intracellular diffusion and by the reduced conductance of the mtOM (Jepihhina *et al.* 2011, Illaste *et al.* 2012, Simson *et al.* 2016), either through interaction with tubulin (Rostovtseva *et al.* 2008) or other intracellular structures (Birkedal *et al.* 2014). In permeabilized muscle fibre bundles of high respiratory capacity, the apparent  $K_m$  for ADP increases up to 0.5 mM (Saks *et al.* 1998), consistent with experimental evidence that >90% saturation is reached only at >5 mM ADP (Pesta and Gnaiger 2012). Similar ADP concentrations are also required for accurate determination of OXPHOS-capacity in human clinical cancer samples and permeabilized cells (Klepinin *et al.* 2016; Koit *et al.* 2017). Whereas 2.5 to 5 mM ADP is sufficient to obtain the actual OXPHOS-capacity in many types of permeabilized tissue and cell preparations, experimental validation is required in each specific case.

**Electron transfer-state (Fig. 5C):** The ET-state is defined as the *noncoupled* state with kinetically-saturating concentrations of O<sub>2</sub>, respiratory substrate and optimum *exogenous* uncoupler concentration for maximum O<sub>2</sub> flux, as an estimate of ET-capacity. Inhibition of respiration is observed at higher than optimum uncoupler concentrations. As a consequence of the nearly collapsed protonmotive force, the driving force is insufficient for phosphorylation, and  $J_P = 0$ .

**ROX state and *Rox*:** Besides the three fundamental coupling states of mitochondrial preparations, the state of residual oxygen consumption, ROX, is relevant to assess respiratory function. ROX is not a coupling state. The rate of residual oxygen consumption, *Rox*, is defined as O<sub>2</sub> consumption due to oxidative side reactions remaining after inhibition of ET—with rotenone, malonic acid and antimycin A. Cyanide and azide not only inhibit CIV but also several peroxidases involved in *Rox*. ROX represents a baseline that is used to correct mitochondrial respiration in defined coupling states. *Rox* is not necessarily equivalent to non-mitochondrial respiration, considering oxygen-consuming reactions in mitochondria not related to ET—such as oxygen consumption in reactions catalyzed by monoamine oxidases (type A and B), monooxygenases (cytochrome P450 monooxygenases), dioxygenase (sulfur dioxygenase and trimethyllysine dioxygenase), and several hydroxylases. Mitochondrial preparations, especially those obtained from liver, may be contaminated by peroxisomes. This fact makes the exact determination of mitochondrial oxygen consumption and mitochondria-associated generation of reactive oxygen species complicated (Schönfeld *et al.* 2009). The dependence of ROX-linked oxygen consumption needs to be studied in detail together with non-ET enzyme activities, availability of specific substrates, oxygen concentration, and electron leakage leading to the formation of reactive oxygen species.

### 2.3. Classical terminology for isolated mitochondria

*‘When a code is familiar enough, it ceases appearing like a code; one forgets that there is a decoding mechanism. The message is identical with its meaning’ (Hofstadter 1979).*

Chance and Williams (1955; 1956) introduced five classical states of mitochondrial respiration and cytochrome redox states. **Table 3** shows a protocol with isolated mitochondria in a closed respirometric chamber, defining a sequence of respiratory states. States and rates are not specifically distinguished in this nomenclature.



**Table 3. Metabolic states of mitochondria (Chance and Williams, 1956; Table V).**

State	[O <sub>2</sub> ]	ADP level	Substrate level	Respiration rate	Rate-limiting substance
1	>0	low	low	slow	ADP
2	>0	high	~0	slow	substrate
3	>0	high	high	fast	respiratory chain
4	>0	low	high	slow	ADP
5	0	high	high	0	oxygen

**State 1** is obtained after addition of isolated mitochondria to air-saturated isoosmotic/isotonic respiration medium containing P<sub>i</sub>, but no fuel substrates and no adenylates, *i.e.*, AMP, ADP, ATP.

**State 2** is induced by addition of a ‘high’ concentration of ADP (typically 100 to 300 μM), which stimulates respiration transiently on the basis of endogenous fuel substrates and phosphorylates only a small portion of the added ADP. State 2 is then obtained at a low respiratory activity limited by exhausted endogenous fuel substrate availability (**Table 3**). If addition of specific inhibitors of respiratory complexes—such as rotenone—does not cause a further decline of oxygen consumption, State 2 is equivalent to the state of residual oxygen consumption, ROX (See below.). If inhibition is observed, undefined endogenous fuel substrates are a confounding factor of pathway control, contributing to the effect of subsequently externally added substrates and inhibitors. In contrast to the original protocol, an alternative sequence of titration steps is frequently applied, in which the alternative ‘State 2’ has an entirely different meaning, when this second state is induced by addition of fuel substrate without ADP (LEAK-state; in contrast to State 2 defined in **Table 1** as a ROX state), followed by addition of ADP.

**State 3** is the state stimulated by addition of fuel substrates while the ADP concentration is still high (**Table 3**) and supports coupled energy transformation through oxidative phosphorylation. ‘High ADP’ is a concentration of ADP specifically selected to allow the measurement of State 3 to State 4 transitions of isolated mitochondria in a closed respirometric chamber. Repeated ADP titration re-establishes State 3 at ‘high ADP’. Starting at oxygen concentrations near air-saturation (ca. 200 μM O<sub>2</sub> at sea level and 37 °C), the total ADP concentration added must be low enough (typically 100 to 300 μM) to allow phosphorylation to ATP at a coupled rate of oxygen consumption that does not lead to oxygen depletion during the transition to State 4. In contrast, kinetically-saturating ADP concentrations usually are 10-fold higher than ‘high ADP’, *e.g.*, 2.5 mM in isolated mitochondria. The abbreviation State 3u is occasionally used in bioenergetics, to indicate the state of respiration after titration of an uncoupler, without sufficient emphasis on the fundamental difference between OXPHOS-capacity (*well-coupled* with an *endogenous* uncoupled component) and ET-capacity (*noncoupled*).

**State 4** is a LEAK-state that is obtained only if the mitochondrial preparation is intact and well-coupled. Depletion of ADP by phosphorylation to ATP leads to a decline in the rate of oxygen consumption in the transition from State 3 to State 4. Under these conditions of State 4, a maximum protonmotive force and high ATP/ADP ratio are maintained. For calculation of P<sub>»</sub>/O<sub>2</sub> ratios the gradual decline of Y<sub>P<sub>»</sub>/O<sub>2</sub></sub> towards diminishing [ADP] at State 4 must be taken into account (Gnaiger 2001). State 4 respiration, L<sub>T</sub> (**Table 1**), reflects intrinsic proton leak and intrinsic ATP hydrolysis activity. Oxygen consumption in State 4 is an overestimation of LEAK-respiration if the contaminating ATP hydrolysis activity recycles some ATP to ADP, J<sub>P<sub>«</sub></sub>, which stimulates respiration coupled to phosphorylation, J<sub>P<sub>»</sub></sub> > 0. This can be tested by inhibition of the phosphorylation-pathway using oligomycin, ensuring that J<sub>P<sub>»</sub></sub> = 0 (State 4o).



Alternatively, sequential ADP titrations re-establish State 3, followed by State 3 to State 4 transitions while sufficient oxygen is available. Anoxia may be reached, however, before exhaustion of ADP (State 5).

**State 5** is the state after exhaustion of oxygen in a closed respirometric chamber. Diffusion of oxygen from the surroundings into the aqueous solution may be a confounding factor preventing complete anoxia (Gnaiger 2001). Chance and Williams (1955) provide an alternative definition of State 5, which gives it the different meaning of ROX versus anoxia: ‘State 5 may be obtained by antimycin A treatment or by anaerobiosis’.

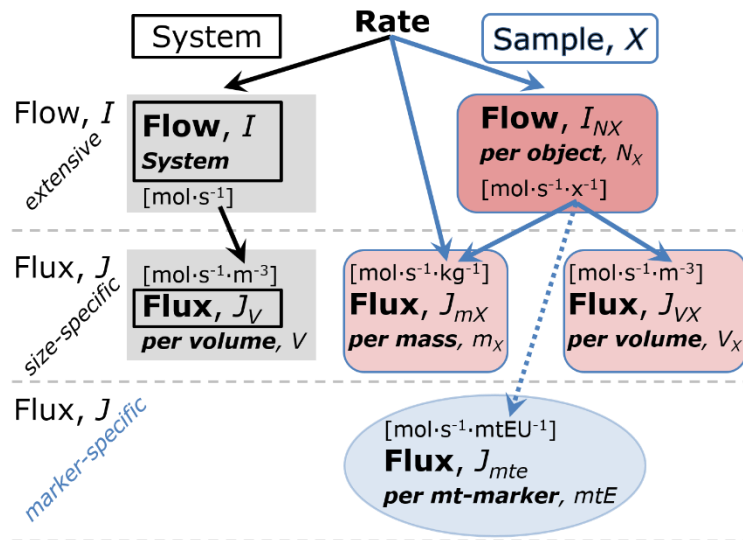
In **Table 3**, only States 3 and 4 (and ‘State 2’ in the alternative protocol: addition of fuel substrates without ADP; not included in the table) are coupling control states, with the restriction that  $O_2$  flux in State 3 may be limited kinetically by non-saturating ADP concentrations (**Table 1**).

### 3. Normalization: fluxes and flows

#### 3.1. Normalization: system or sample

The term *rate* is not sufficiently defined to be useful for reporting data (**Fig. 6**). The inconsistency of the meanings of rate becomes fully apparent when considering Galileo Galilei’s famous principle, that ‘bodies of different weight all fall at the same rate (have a constant acceleration)’ (Coopersmith 2010).

**Fig. 6. Different meanings of rate may lead to confusion, if the normalization is not sufficiently specified.** Results are frequently expressed as mass-specific *flux*,  $J_{mX}$ , per mg protein, dry or wet weight (mass). Cell volume,  $V_{cell}$ , may be used for normalization (volume-specific flux,  $J_{Vcell}$ ), which must be clearly distinguished from flow per cell,  $I_{Ncell}$ , or flux,  $J_V$ , expressed for methodological reasons per volume of the measurement system. For details see **Table 4**.



**Flow per system,  $I$ :** In a generalization of electrical terms, flow as an extensive quantity ( $I$ ; per system) is distinguished from flux as a size-specific quantity ( $J$ ; per system size) (**Fig. 6**). Electric current is flow,  $I_{el}$  [ $A \equiv C \cdot s^{-1}$ ] per system (extensive quantity). When dividing this extensive quantity by system size (cross-sectional area of a ‘wire’), a size-specific quantity is obtained, which is flux (current density),  $J_{el}$  [ $A \cdot m^{-2} = C \cdot s^{-1} \cdot m^{-2}$ ].

**Extensive quantities:** An extensive quantity increases proportionally with system size. The magnitude of an extensive quantity is completely additive for non-interacting subsystems—such as mass or flow expressed per defined system. The magnitude of these quantities depends on the extent or size of the system (Cohen *et al.* 2008).

**Size-specific quantities:** ‘The adjective *specific* before the name of an extensive quantity is often used to mean *divided by mass*’ (Cohen *et al.* 2008). In this system-paradigm, mass-specific flux is flow divided by mass of the *system* (the total mass of everything within the measuring chamber or reactor). A mass-specific quantity is independent of the extent of non-

interacting homogenous subsystems. Tissue-specific quantities (related to the *sample* in contrast to the *system*) are of fundamental interest in comparative mitochondrial physiology, where *specific* refers to the *type of the sample* rather than *mass of the system*. The term *specific*, therefore, must be clarified; *sample-specific*, e.g., muscle mass-specific normalization, is distinguished from *system-specific* quantities (mass or volume; **Fig. 6**).

---

## Box 2: Metabolic fluxes and flows: vectorial and scalar

---

Fluxes are *vectors*, if they have *spatial* geometric direction in addition to magnitude. Electric charge per unit time is electric flow or current,  $I_{el} = dQ_{el} \cdot dt^{-1}$  [A]. When expressed per unit cross-sectional area,  $A$  [m<sup>2</sup>], a vector flux is obtained, which is current density or surface-density of flow) perpendicular to the direction of flux,  $J_{el} = I_{el} \cdot A^{-1}$  [A·m<sup>-2</sup>] (Cohen et al. 2008). For all transformations *flows*,  $I_{tr}$ , are defined as extensive quantities. Vector and scalar *fluxes* are obtained as  $J_{tr} = I_{tr} \cdot A^{-1}$  [mol·s<sup>-1</sup>·m<sup>-2</sup>] and  $J_{tr} = I_{tr} \cdot V^{-1}$  [mol·s<sup>-1</sup>·m<sup>-3</sup>], expressing flux as an area-specific vector or volume-specific vectorial or scalar quantity, respectively (Gnaiger 1993b).

We suggest to define: (1) *vectorial* fluxes, which are translocations as functions of *gradients* with direction in geometric space in continuous systems; (2) *vectorial* fluxes, which describe translocations in discontinuous systems and are restricted to information on *compartmental differences* (**Fig. 2**, transmembrane proton flux); and (3) *scalar* fluxes, which are transformations in a *homogenous* system (**Fig. 2**, catabolic O<sub>2</sub> flux,  $J_{kO_2}$ ).

Vectorial transmembrane proton fluxes,  $J_{mH+pos}$  and  $J_{mH+neg}$ , are analyzed in a heterogenous compartmental system as a quantity with *directional* but not *spatial* information. Translocation of protons across the mtIM has a defined direction, either from the negative compartment (matrix space; negative, neg-compartment) to the positive compartment (intermembrane space; positive, pos-compartment) or *vice versa* (**Fig. 2**). The arrows defining the direction of the translocation between the two compartments may point upwards or downwards, right or left, without any implication that these are actual directions in space. The pos-compartment is neither above nor below the neg-compartment in a spatial sense, but can be visualized arbitrarily in a figure in the upper position (**Fig. 2**). In general, the *compartmental direction* of vectorial translocation from the neg-compartment to the pos-compartment is defined by assigning the initial and final state as *ergodynamic compartments*,  $H_{neg}^+ \rightarrow H_{pos}^+$  or  $0 = -1 H_{neg}^+ + 1 H_{pos}^+$ , related to work (erg = work) that must be performed to lift the proton from a lower to a higher electrochemical potential or from the lower to the higher ergodynamic compartment (Gnaiger 1993b).

In analogy to *vectorial* translocation, the direction of a *scalar* chemical reaction,  $A \rightarrow B$  or  $0 = -1 A + 1 B$ , is defined by assigning substrates and products, A and B, as ergodynamic compartments. O<sub>2</sub> is defined as a substrate in respiratory O<sub>2</sub> consumption, which together with the fuel substrates comprises the substrate compartment of the catabolic reaction (**Fig. 2**). Volume-specific scalar O<sub>2</sub> flux is coupled to vectorial translocation, yielding the  $H_{pos}^+/O_2$  ratio (**Fig. 1**).

---

### 3.2. Normalization for system-size: flux per chamber volume

**System-specific flux,  $J_{V,O_2}$ :** The experimental system (experimental chamber) is part of the measurement apparatus, separated from the environment as an isolated, closed, open, isothermal or non-isothermal system (**Table 4**). On another level, we distinguish between (1) the *system* with volume  $V$  and mass  $m$  defined by the system boundaries, and (2) the *sample* or *objects* with volume  $V_X$  and mass  $m_X$  which are enclosed in the experimental chamber (**Fig. 6**). Metabolic O<sub>2</sub> flow per object,  $I_{O_2/X}$ , increases as the mass of the object is increased. Sample mass-specific O<sub>2</sub> flux,  $J_{O_2/mX}$  should be independent of the mass of the sample studied in the

instrument chamber, but system volume-specific O<sub>2</sub> flux,  $J_{V,O_2}$  (per volume of the instrument chamber), should increase in direct proportion to the mass of the sample in the chamber. Whereas  $J_{V,O_2}$  depends on mass-concentration of the sample in the chamber, it should be independent of the chamber (system) volume at constant sample mass. There are practical limitations to increase the mass-concentration of the sample in the chamber, when one is concerned about crowding effects and instrumental time resolution.

When the reactor volume does not change during the reaction, which is typical for liquid phase reactions, the volume-specific *flux of a chemical reaction*  $r$  is the time derivative of the advancement of the reaction per unit volume,  $J_{V,rB} = d\zeta_B/dt \cdot V^{-1}$  [(mol·s<sup>-1</sup>)·L<sup>-1</sup>]. The *rate of concentration change* is  $dc_B/dt$  [(mol·L<sup>-1</sup>)·s<sup>-1</sup>], where concentration is  $c_B = n_B/V$ . There is a difference between (1)  $J_{V,rO_2}$  [mol·s<sup>-1</sup>·L<sup>-1</sup>] and (2) rate of concentration change [mol·L<sup>-1</sup>·s<sup>-1</sup>]. These merge to a single expression only in closed systems. In open systems, external fluxes (such as O<sub>2</sub> supply) are distinguished from internal transformations (catabolic flux, O<sub>2</sub> consumption). In a closed system, external flows of all substances are zero and O<sub>2</sub> consumption (internal flow of catabolic reactions  $k$ ),  $I_{kO_2}$  [pmol·s<sup>-1</sup>], causes a decline of the amount of O<sub>2</sub> in the system,  $n_{O_2}$  [nmol]. Normalization of these quantities for the volume of the system,  $V$  [L ≡ dm<sup>3</sup>], yields volume-specific O<sub>2</sub> flux,  $J_{V,kO_2} = I_{kO_2}/V$  [nmol·s<sup>-1</sup>·L<sup>-1</sup>], and O<sub>2</sub> concentration,  $[O_2]$  or  $c_{O_2} = n_{O_2}/V$  [μmol·L<sup>-1</sup> = μM = nmol·mL<sup>-1</sup>]. Instrumental background O<sub>2</sub> flux is due to external flux into a non-ideal closed respirometer; then total volume-specific flux has to be corrected for instrumental background O<sub>2</sub> flux—O<sub>2</sub> diffusion into or out of the instrumental chamber.  $J_{V,kO_2}$  is relevant mainly for methodological reasons and should be compared with the accuracy of instrumental resolution of background-corrected flux, e.g., ±1 nmol·s<sup>-1</sup>·L<sup>-1</sup> (Gnaiger 2001). ‘Metabolic’ or catabolic indicates O<sub>2</sub> flux,  $J_{kO_2}$ , corrected for: (1) instrumental background O<sub>2</sub> flux; (2) chemical background O<sub>2</sub> flux due to autoxidation of chemical components added to the incubation medium; and (3)  $R_{ox}$  for O<sub>2</sub>-consuming side reactions unrelated to the catabolic pathway  $k$ .

### 3.3. Normalization: per sample

The challenges of measuring mitochondrial respiratory flux are matched by those of normalization. Application of common and defined units is required for direct transfer of reported results into a database. The second [s] is the *SI* unit for the base quantity *time*. It is also the standard time-unit used in solution chemical kinetics. A rate may be considered as the numerator and normalization as the complementary denominator, which are tightly linked in reporting the measurements in a format commensurate with the requirements of a database. Normalization (Table 4) is guided by physicochemical principles, methodological considerations, and conceptual strategies (Fig. 7).

**Sample concentration,  $C_{mX}$ :** Normalization for sample concentration is required to report respiratory data. Considering a tissue or cells as the sample,  $X$ , the sample mass is  $m_X$  [mg], which is frequently measured as wet or dry weight,  $W_w$  or  $W_d$  [mg], or as amount of tissue or cell protein,  $m_{\text{protein}}$ . In the case of permeabilized tissues, cells, and homogenates, the sample concentration,  $C_{mX} = m_X/V$  [g·L<sup>-1</sup> = mg·mL<sup>-1</sup>], is the mass of the subsample of tissue that is transferred into the instrument chamber.

**Mass-specific flux,  $J_{O_2/mX}$ :** Mass-specific flux is obtained by expressing respiration per mass of sample,  $m_X$  [mg].  $X$  is the type of sample—isolated mitochondria, tissue homogenate, permeabilized fibres or cells. Volume-specific flux is divided by mass concentration of  $X$ ,  $J_{O_2/mX} = J_{V,O_2}/C_{mX}$ ; or flow per cell is divided by mass per cell,  $J_{O_2/mcell} = I_{O_2/cell}/M_{\text{cell}}$ . If mass-specific O<sub>2</sub> flux is constant and independent of sample size (expressed as mass), then there is no interaction between the subsystems. A 1.5 mg and a 3.0 mg muscle sample respire at identical mass-specific flux. Mass-specific O<sub>2</sub> flux, however, may change with the mass of a tissue sample, cells or isolated mitochondria in the measuring chamber, in which the nature of the

interaction becomes an issue. Therefore, cell density must be optimization, particularly in experiments carried out in wells, considering the confluency of the cell monolayer or clumps of cells (Salabei *et al.* 2014).

**Number concentration,  $C_{NX}$ :**  $C_{NX}$  is the experimental *number concentration* of sample  $X$ . In the case of cells or animals, *e.g.*, nematodes,  $C_{NX} = N_X/V [X \cdot L^{-1}]$ , where  $N_X$  is the number of cells or organisms in the chamber (**Table 4**).

**Table 4. Sample concentrations and normalization of flux.**

Expression	Symbol	Definition	Unit	Notes
<b>Sample</b>				
identity of sample	$X$	object: cell, tissue, animal, patient		
number of sample entities $X$	$N_X$	number of objects	x	
mass of sample $X$	$m_X$		kg	1
mass of object $X$	$M_X$	$M_X = m_X \cdot N_X^{-1}$	kg·x <sup>-1</sup>	1
<b>Mitochondria</b>				
mitochondria	mt	$X = \text{mt}$		
amount of mt-elements	$mtE$	quantity of mt-marker	mtEU	
<b>Concentrations</b>				
object number concentration	$C_{NX}$	$C_{NX} = N_X \cdot V^{-1}$	x·m <sup>-3</sup>	2
sample mass concentration	$C_{mX}$	$C_{mX} = m_X \cdot V^{-1}$	kg·m <sup>-3</sup>	
mitochondrial concentration	$C_{mtE}$	$C_{mtE} = mtE \cdot V^{-1}$	mtEU·m <sup>-3</sup>	3
specific mitochondrial density	$D_{mtE}$	$D_{mtE} = mtE \cdot m_X^{-1}$	mtEU·kg <sup>-1</sup>	4
mitochondrial content, $mtE$ per object $X$	$mtE_X$	$mtE_X = mtE \cdot N_X^{-1}$	mtEU·x <sup>-1</sup>	5
<b>O<sub>2</sub> flow and flux</b>				
flow, system	$I_{O_2}$	internal flow	mol·s <sup>-1</sup>	6
volume-specific flux	$J_{V,O_2}$	$J_{V,O_2} = I_{O_2} \cdot V^{-1}$	mol·s <sup>-1</sup> ·m <sup>-3</sup>	7
flow per object $X$	$I_{O_2/X}$	$I_{O_2/X} = J_{V,O_2} \cdot C_{NX}^{-1}$	mol·s <sup>-1</sup> ·x <sup>-1</sup>	8
mass-specific flux	$J_{O_2/mX}$	$J_{O_2/mX} = J_{V,O_2} \cdot C_{mX}^{-1}$	mol·s <sup>-1</sup> ·kg <sup>-1</sup>	9
mitochondria-specific flux	$J_{O_2/mtE}$	$J_{O_2/mtE} = J_{V,O_2} \cdot C_{mtE}^{-1}$	mol·s <sup>-1</sup> ·mtEU <sup>-1</sup>	10

- The SI prefix k is used for the SI base unit of mass (kg = 1,000 g). In praxis, various SI prefixes are used for convenience, to make numbers easily readable, *e.g.*, 1 mg tissue, cell or mitochondrial mass instead of 0.000001 kg.
- In case sample  $X = \text{cells}$ , the object number concentration is  $C_{N\text{cell}} = N_{\text{cell}} \cdot V^{-1}$ , and volume may be expressed in [dm<sup>3</sup> ≡ L] or [cm<sup>3</sup> = mL]. See **Table 5** for different object types.
- mt-concentration is an experimental variable, dependent on sample concentration: (1)  $C_{mtE} = mtE \cdot V^{-1}$ ; (2)  $C_{mtE} = mtE_X \cdot C_{NX}$ ; (3)  $C_{mtE} = C_{mX} \cdot D_{mtE}$ .
- If the amount of mitochondria,  $mtE$ , is expressed as mitochondrial mass, then  $D_{mtE}$  is the mass fraction of mitochondria in the sample. If  $mtE$  is expressed as mitochondrial volume,  $V_{mt}$ , and the mass of sample,  $m_X$ , is replaced by volume of sample,  $V_X$ , then  $D_{mtE}$  is the volume fraction of mitochondria in the sample.
- $mtE_X = mtE \cdot N_X^{-1} = C_{mtE} \cdot C_{NX}^{-1}$ .
- O<sub>2</sub> can be replaced by other chemicals B to study different reactions, *e.g.*, ATP, H<sub>2</sub>O<sub>2</sub>, or compartmental translocations, *e.g.*, Ca<sup>2+</sup>.
- $I_{O_2}$  and  $V$  are defined per instrument chamber as a system of constant volume (and constant temperature), which may be closed or open.  $I_{O_2}$  is abbreviated for  $I_{rO_2}$ , *i.e.*, the metabolic or internal O<sub>2</sub> flow of the chemical reaction  $r$  in which O<sub>2</sub> is consumed, hence the negative stoichiometric number,  $\nu_{O_2} = -1$ .  $I_{rO_2} = d_r n_{O_2} / dt \cdot \nu_{O_2}^{-1}$ . If  $r$  includes all chemical reactions in which O<sub>2</sub> participates, then  $d_r n_{O_2} = dn_{O_2} - d_e n_{O_2}$ , where  $dn_{O_2}$  is the change in the amount of O<sub>2</sub> in the instrument chamber and  $d_e n_{O_2}$



is the amount of  $O_2$  added externally to the system. At steady state, by definition  $dn_{O_2} = 0$ , hence  $d_t n_{O_2} = -d_e n_{O_2}$ .

8  $J_{V,O_2}$  is an experimental variable, expressed per volume of the instrument chamber.

9  $I_{O_2/X}$  is a physiological variable, depending on the size of entity  $X$ .

10 There are many ways to normalize for a mitochondrial marker, that are used in different experimental approaches: (1)  $J_{O_2/mtE} = J_{V,O_2} \cdot C_{mtE}^{-1}$ ; (2)  $J_{O_2/mtE} = J_{V,O_2} \cdot C_{mX}^{-1} \cdot D_{mtE}^{-1} = J_{O_2/mX} \cdot D_{mtE}^{-1}$ ; (3)  $J_{O_2/mtE} = J_{V,O_2} \cdot C_{NX}^{-1} \cdot mtE_X^{-1} = I_{O_2/X} \cdot mtE_X^{-1}$ ; (4)  $J_{O_2/mtE} = I_{O_2} \cdot mtE^{-1}$ . The mt-elemental unit [mtEU] varies between different mt-markers.

**Table 5. Sample types,  $X$ , abbreviations, and quantification.**

Identity of sample	$X$	$N_X$	Mass <sup>a</sup>	Volume	mt-Marker
mitochondrial preparation	Mtprep	[x]	[kg]	[m <sup>3</sup> ]	[mtEU]
isolated mitochondria	imt		$m_{mt}$	$V_{mt}$	$mtE$
tissue homogenate	thom		$m_{thom}$		$mtE_{thom}$
permeabilized tissue	pti		$m_{pti}$		$mtE_{pti}$
permeabilized fibre	pfi		$m_{pfi}$		$mtE_{pfi}$
permeabilized cell	pce	$N_{pce}$	$M_{pce}$	$V_{pce}$	$mtE_{pce}$
intact cell	ce	$N_{ce}$	$M_{ce}$	$V_{ce}$	$mtE_{ce}$
Organism	org	$N_{org}$	$M_{org}$	$V_{org}$	

<sup>a</sup> Instead of mass, frequently the wet weight or dry weight is stated,  $W_w$  or  $W_d$ .

$m_X$  is mass of the sample [kg],  $M_X$  is mass of the object [kg·x<sup>-1</sup>].

**Flow per object,  $I_{O_2/X}$ :** A special case of normalization is encountered in respiratory studies with permeabilized (or intact) cells. If respiration is expressed per cell, the  $O_2$  flow per measurement system is replaced by the  $O_2$  flow per cell,  $I_{O_2/cell}$  (Table 4).  $O_2$  flow can be calculated from volume-specific  $O_2$  flux,  $J_{V,O_2}$  [nmol·s<sup>-1</sup>·L<sup>-1</sup>] (per  $V$  of the measurement chamber [L]), divided by the number concentration of cells,  $C_{Nce} = N_{ce}/V$  [cell·L<sup>-1</sup>], where  $N_{ce}$  is the number of cells in the chamber. Cellular  $O_2$  flow can be compared between cells of identical size. To take into account changes and differences in cell size, normalization is required to obtain cell size-specific or mitochondrial marker-specific  $O_2$  flux (Renner *et al.* 2003).

The complexity changes when the sample is a whole organism studied as an experimental model. The scaling law in respiratory physiology reveals a strong interaction of  $O_2$  consumption and individual body mass of an organism, since *basal* metabolic rate (flow) does not increase linearly with body mass, whereas *maximum* mass-specific  $O_2$  flux,  $\dot{V}_{O_2max}$  or  $\dot{V}_{O_2peak}$ , is approximately constant across a large range of individual body mass (Weibel and Hoppeler 2005), with individuals, breeds, and species deviating substantially from this relationship.  $\dot{V}_{O_2peak}$  of human endurance athletes is 60 to 80 mL  $O_2$ ·min<sup>-1</sup>·kg<sup>-1</sup> body mass, converted to  $J_{M,O_2peak}$  of 45 to 60 nmol·s<sup>-1</sup>·g<sup>-1</sup> (Gnaiger 2014; Table 6).

### 3.4. Normalization for mitochondrial content

Tissues can contain multiple cell populations that may have distinct mitochondrial subtypes. Mitochondria undergo dynamic fission and fusion cycles, and can exist in multiple stages and sizes which may be altered by a range of factors. The isolation of mitochondria (often achieved through differential centrifugation) can therefore yield a subsample of the mitochondrial types present in a tissue, depending on isolation protocols utilized (*e.g.*, centrifugation speed). This possible bias should be taken into account when planning experiments using isolated mitochondria. Different sizes of mitochondria are enriched at specific centrifugation speeds, which is used for isolation of mitochondrial subpopulations.

Part of the mitochondrial content of a tissue is lost during preparation of isolated mitochondria. The fraction of mitochondria in the isolate is expressed as mitochondrial recovery. At a high mitochondrial recovery the sample of isolated mitochondria is more representative of the total mitochondrial population than in preparations characterized by low



recovery. Determination of the mitochondrial recovery and yield is based on measurement of the concentration of a mitochondrial marker in the tissue homogenate,  $C_{mtE,thom}$ , which simultaneously provides information on the specific mitochondrial density in the sample.

Normalization is a problematic subject; it is essential to consider the question of the study. If the study aims at comparing tissue performance—such as the effects of a treatment on a specific tissue, then normalization can be successful, using tissue mass or protein content, for example. However, if the aim is to find differences on mitochondrial function independent of mitochondrial density (Table 4), then normalization to a mitochondrial marker is imperative (Fig. 7). One cannot assume that quantitative changes in various markers—such as mitochondrial proteins—necessarily occur in parallel with one another. It should be established that the marker chosen is not selectively altered by the performed treatment. In conclusion, the normalization must reflect the question under investigation to reach a satisfying answer. On the other hand, the goal of comparing results across projects and institutions requires standardization on normalization for entry into a databank.

<b>Flow, Performance</b>	=	<b>Element function</b>	x	<b>Element density</b>	x	<b>Size of object</b>
$\frac{\text{mol} \cdot \text{s}^{-1}}{x}$	=	$\frac{\text{mol} \cdot \text{s}^{-1}}{x_{mtE}}$	·	$\frac{x_{mtE}}{\text{kg}}$	·	$\frac{\text{kg}}{x}$

A

<b>Flow</b>	=	<b>mt-specific flux</b>	x	<b>mt-structure, functional elements</b>
$I_{O_2/X}$	=	$J_{O_2/mtE}$	·	$mtE_X$
				$\frac{mtE_X}{M_X} \cdot M_X$

B

$I_{O_2/X}$	=	$J_{O_2/mtE}$	·	$D_{mtE}$	·	$M_X$
				$\frac{I_{O_2/X}}{M_X}$	·	$\frac{mtE_X}{M_X}$

B

$I_{O_2/X}$	=	$J_{O_2/MX}$	·	$M_X$
<b>Flow</b>	=	<b>Object mass- specific flux</b>	x	<b>Mass of object</b>

**Fig. 7. Structure-function analysis of performance of an organism, organ or tissue, or a cell (sample entity, X).  $O_2$  flow,  $I_{O_2/X}$ , is the product of performance per functional element (element function, mitochondria-specific flux), element density (mitochondrial density,  $D_{mtE}$ ), and size of entity X (mass,  $M_X$ ). (A) Structured analysis: performance is the product of mitochondrial function (mt-specific flux) and structure (functional elements;  $D_{mtE}$  times mass of X). (B) Unstructured analysis: performance is the product of entity mass-specific flux,  $J_{O_2/MX} = I_{O_2/X}/M_X = I_{O_2}/m_X$  [ $\text{mol} \cdot \text{s}^{-1} \cdot \text{kg}^{-1}$ ] and size of entity, expressed as mass of X;  $M_X = m_X \cdot N_X^{-1}$  [ $\text{kg} \cdot \text{x}^{-1}$ ]. See Table 4 for further explanation of quantities and units. Modified from Gnaiger (2014).**

**Mitochondrial concentration,  $C_{mtE}$ , and mitochondrial markers:** Mitochondrial organelles comprise a dynamic cellular reticulum in various states of fusion and fission. Hence, the definition of an "amount" of mitochondria is often misconceived: mitochondria cannot be counted reliably as a number of occurring elements. Therefore, quantification of the "amount" of mitochondria depends on the measurement of chosen mitochondrial markers. 'Mitochondria are the structural and functional elemental units of cell respiration' (Gnaiger 2014). The quantity of a mitochondrial marker can reflect the amount of *mitochondrial elements*,  $mtE$ ,

expressed in various mitochondrial elemental units [mtEU] specific for each measured mt-marker (**Table 4**). However, since mitochondrial quality may change in response to stimuli—particularly in mitochondrial dysfunction and after exercise training (Pesta *et al.* 2011; Campos *et al.* 2017)—some markers can vary while others are unchanged: (1) Mitochondrial volume and membrane area are structural markers, whereas mitochondrial protein mass is frequently used as a marker for isolated mitochondria. (2) Molecular and enzymatic mitochondrial markers (amounts or activities) can be selected as matrix markers, *e.g.*, citrate synthase activity, mtDNA; mtIM-markers, *e.g.*, cytochrome *c* oxidase activity, *aa*<sub>3</sub> content, cardiolipin, or mtOM-markers, *e.g.*, TOM20. (3) Extending the measurement of mitochondrial marker enzyme activity to mitochondrial pathway capacity, ET- or OXPHOS-capacity can be considered as an integrative functional mitochondrial marker.

Depending on the type of mitochondrial marker, the mitochondrial elements, *mtE*, are expressed in marker-specific units. Mitochondrial concentration in the measurement chamber and the tissue of origin are quantified as (1) a quantity for normalization in functional analyses,  $C_{mtE}$ , and (2) a physiological output that is the result of mitochondrial biogenesis and degradation,  $D_{mtE}$ , respectively (**Table 4**). It is recommended, therefore, to distinguish *experimental mitochondrial concentration*,  $C_{mtE} = mtE/V$  and *physiological mitochondrial density*,  $D_{mtE} = mtE/m_X$ . Then mitochondrial density is the amount of mitochondrial elements per mass of tissue, which is a biological variable (**Fig. 7**). The experimental variable is mitochondrial density multiplied by sample mass concentration in the measuring chamber,  $C_{mtE} = D_{mtE} \cdot C_{mX}$ , or mitochondrial content multiplied by sample number concentration,  $C_{mtE} = mtE_X \cdot C_{NX}$  (**Table 4**).

**Mitochondria-specific flux,  $J_{O_2/mtE}$ :** Volume-specific metabolic O<sub>2</sub> flux depends on: (1) the sample concentration in the volume of the instrument chamber,  $C_{mX}$ , or  $C_{NX}$ ; (2) the mitochondrial density in the sample,  $D_{mtE} = mtE/m_X$  or  $mtE_X = mtE/N_X$ ; and (3) the specific mitochondrial activity or performance per elemental mitochondrial unit,  $J_{O_2/mtE} = J_{V,O_2}/C_{mtE}$  [mol·s<sup>-1</sup>·mtEU<sup>-1</sup>] (**Table 4**). Obviously, the numerical results for  $J_{O_2/mtE}$  vary with the type of mitochondrial marker chosen for measurement of *mtE* and  $C_{mtE} = mtE/V$  [mtEU·m<sup>-3</sup>].

### 3.5. Evaluation of mitochondrial markers

Different methods are implicated in the quantification of mitochondrial markers and have different strengths. Some problems are common for all mitochondrial markers, *mtE*: (1) Accuracy of measurement is crucial, since even a highly accurate and reproducible measurement of O<sub>2</sub> flux results in an inaccurate and noisy expression normalized for a biased and noisy measurement of a mitochondrial marker. This problem is acute in mitochondrial respiration because the denominators used (the mitochondrial markers) are often small moieties of which accurate and precise determination is difficult. This problem can be avoided when O<sub>2</sub> fluxes measured in substrate-uncoupler-inhibitor titration protocols are normalized for flux in a defined respiratory reference state, which is used as an *internal* marker and yields flux control ratios, *FCRs*. *FCRs* are independent of any *externally* measured markers and, therefore, are statistically robust, considering the limitations of ratios in general (Jasienski and Bazzaz 1999). *FCRs* indicate qualitative changes of mitochondrial respiratory control, with highest quantitative resolution, separating the effect of mitochondrial density or concentration on  $J_{O_2/mX}$  and  $I_{O_2/X}$  from that of function per elemental mitochondrial marker,  $J_{O_2/mtE}$  (Pesta *et al.* 2011; Gnaiger 2014). (2) If mitochondrial quality does not change and only the amount of mitochondria varies as a determinant of mass-specific flux, any marker is equally qualified in principle; then in practice selection of the optimum marker depends only on the accuracy and precision of measurement of the mitochondrial marker. (3) If mitochondrial flux control ratios change, then there may not be any best mitochondrial marker. In general, measurement of multiple mitochondrial markers enables a comparison and evaluation of normalization for a

variety of mitochondrial markers. Particularly during postnatal development, the activity of marker enzymes—such as cytochrome *c* oxidase and citrate synthase—follows different time courses (Drahota *et al.* 2004). Evaluation of mitochondrial markers in healthy controls is insufficient for providing guidelines for application in the diagnosis of pathological states and specific treatments.

In line with the concept of the respiratory control ratio (Chance and Williams 1955a), the most readily used normalization is that of flux control ratios and flux control factors (Gnaiger 2014). Selection of the state of maximum flux in a protocol as the reference state has the advantages of: (1) internal normalization; (2) statistical linearization of the response in the range of 0 to 1; and (3) consideration of maximum flux for integrating a large number of elemental steps in the OXPHOS- or ET-pathways. This reduces the risk of selecting a functional marker that is specifically altered by the treatment or pathology, yet increases the chance that the highly integrative pathway is disproportionately affected, *e.g.*, the OXPHOS- rather than ET-pathway in case of an enzymatic defect in the phosphorylation-pathway. In this case, additional information can be obtained by reporting flux control ratios based on a reference state which indicates stable tissue-mass specific flux. Stereological determination of mitochondrial content via two-dimensional transmission electron microscopy can have limitations due to the dynamics of mitochondrial size (Meinild Lundby *et al.* 2017). Accurate determination of three-dimensional volume by two-dimensional microscopy can be both time consuming and statistically challenging (Larsen *et al.* 2012).

The validity of using mitochondrial marker enzymes (citrate synthase activity, Complex I–IV amount or activity) for normalization of flux is limited in part by the same factors that apply to flux control ratios. Strong correlations between various mitochondrial markers and citrate synthase activity (Reichmann *et al.* 1985; Boushel *et al.* 2007; Mogensen *et al.* 2007) are expected in a specific tissue of healthy subjects and in disease states not specifically targeting citrate synthase. Citrate synthase activity is acutely modifiable by exercise (Tonkonogi *et al.* 1997; Leek *et al.* 2001). Evaluation of mitochondrial markers related to a selected age and sex cohort cannot be extrapolated to provide recommendations for normalization in respirometric diagnosis of disease, in different states of development and ageing, different cell types, tissues, and species. mtDNA normalized to nDNA via qPCR is correlated to functional mitochondrial markers including OXPHOS- and ET-capacity in some cases (Puntschart *et al.* 1995; Wang *et al.* 1999; Menshikova *et al.* 2006; Boushel *et al.* 2007), but lack of such correlations have been reported (Menshikova *et al.* 2005; Schultz and Wiesner 2000; Pesta *et al.* 2011). Several studies indicate a strong correlation between cardiolipin content and increase in mitochondrial function with exercise (Menshikova *et al.* 2005; Menshikova *et al.* 2007; Larsen *et al.* 2012; Faber *et al.* 2014), but its use as a general mitochondrial biomarker in disease remains questionable.

### 3.6. Conversion: units

Many different units have been used to report the rate of oxygen consumption, OCR (Table 6). *SI* base units provide the common reference to introduce the theoretical principles (Fig. 6), and are used with appropriately chosen *SI* prefixes to express numerical data in the most practical format, with an effort towards unification within specific areas of application (Table 7). Reporting data in *SI* units—including the mole [mol], coulomb [C], joule [J], and second [s]—should be encouraged, particularly by journals which propose the use of *SI* units.

Although volume is expressed as  $\text{m}^3$  using the *SI* base unit, the litre [ $\text{dm}^3$ ] is a conventional unit of volume for concentration and is used for most solution chemical kinetics. If one multiplies  $I_{\text{O}_2/\text{cell}}$  by  $C_{\text{Ncell}}$ , then the result will not only be the amount of  $\text{O}_2$  [mol] consumed per time [ $\text{s}^{-1}$ ] in one litre [ $\text{L}^{-1}$ ], but also the change in the concentration of oxygen per second (for any volume of an ideally closed system). This is ideal for kinetic modeling as it

blends with chemical rate equations where concentrations are typically expressed in  $\text{mol}\cdot\text{L}^{-1}$  (Wagner *et al.* 2011). In studies of multinuclear cells—such as differentiated skeletal muscle cells—it is easy to determine the number of nuclei but not the total number of cells. A generalized concept, therefore, is obtained by substituting cells by nuclei as the sample entity. This does not hold, however, for enucleated platelets.

**Table 6. Conversion of various units used in respirometry and ergometry.**  $e^-$  is the number of electrons or reducing equivalents.  $z_B$  is the charge number of entity B.

1 Unit	x	Multiplication factor	SI-unit	Note
$\text{ng}\cdot\text{atom O}\cdot\text{s}^{-1}$	(2 $e^-$ )	0.5	$\text{nmol O}_2\cdot\text{s}^{-1}$	
$\text{ng}\cdot\text{atom O}\cdot\text{min}^{-1}$	(2 $e^-$ )	8.33	$\text{pmol O}_2\cdot\text{s}^{-1}$	
$\text{natom O}\cdot\text{min}^{-1}$	(2 $e^-$ )	8.33	$\text{pmol O}_2\cdot\text{s}^{-1}$	
$\text{nmol O}_2\cdot\text{min}^{-1}$	(4 $e^-$ )	16.67	$\text{pmol O}_2\cdot\text{s}^{-1}$	
$\text{nmol O}_2\cdot\text{h}^{-1}$	(4 $e^-$ )	0.2778	$\text{pmol O}_2\cdot\text{s}^{-1}$	
$\text{mL O}_2\cdot\text{min}^{-1}$ at STPD <sup>a</sup>		0.744	$\mu\text{mol O}_2\cdot\text{s}^{-1}$	1
$W = \text{J/s}$ at $-470 \text{ kJ/mol O}_2$		-2.128	$\mu\text{mol O}_2\cdot\text{s}^{-1}$	
$\text{mA} = \text{mC}\cdot\text{s}^{-1}$	( $z_{\text{H}^+} = 1$ )	10.36	$\text{nmol H}^+\cdot\text{s}^{-1}$	2
$\text{mA} = \text{mC}\cdot\text{s}^{-1}$	( $z_{\text{O}_2} = 4$ )	2.59	$\text{nmol O}_2\cdot\text{s}^{-1}$	2
$\text{nmol H}^+\cdot\text{s}^{-1}$	( $z_{\text{H}^+} = 1$ )	0.09649	$\text{mA}$	3
$\text{nmol O}_2\cdot\text{s}^{-1}$	( $z_{\text{O}_2} = 4$ )	0.38594	$\text{mA}$	3

1 At standard temperature and pressure dry (STPD: 0 °C = 273.15 K and 1 atm = 101.325 kPa = 760 mmHg), the molar volume of an ideal gas,  $V_m$ , and  $V_{m,\text{O}_2}$  is 22.414 and 22.392  $\text{L}\cdot\text{mol}^{-1}$ , respectively. Rounded to three decimal places, both values yield the conversion factor of 0.744. For comparison at NTPD (20 °C),  $V_{m,\text{O}_2}$  is 24.038  $\text{L}\cdot\text{mol}^{-1}$ . Note that the SI standard pressure is 100 kPa.

2 The multiplication factor is  $10^6/(z_B\cdot F)$ .

3 The multiplication factor is  $z_B\cdot F/10^6$ .

For studies of cells, we recommend that respiration be expressed, as far as possible, as: (1)  $\text{O}_2$  flux normalized for a mitochondrial marker, for separation of the effects of mitochondrial quality and content on cell respiration (this includes FCRs as a normalization for a functional mitochondrial marker); (2)  $\text{O}_2$  flux in units of cell volume or mass, for comparison of respiration of cells with different cell size (Renner *et al.* 2003) and with studies on tissue preparations, and (3)  $\text{O}_2$  flow in units of attomole ( $10^{-18} \text{ mol}$ ) of  $\text{O}_2$  consumed in a second by each cell [ $\text{amol}\cdot\text{s}^{-1}\cdot\text{cell}^{-1}$ ], numerically equivalent to [ $\text{pmol}\cdot\text{s}^{-1}\cdot 10^{-6} \text{ cells}$ ]. This convention allows information to be easily used when designing experiments in which oxygen consumption must be considered. For example, to estimate the volume-specific  $\text{O}_2$  flux in an instrument chamber that would be expected at a particular cell number concentration, one simply needs to multiply the flow per cell by the number of cells per volume of interest. This provides the amount of  $\text{O}_2$  [mol] consumed per time [ $\text{s}^{-1}$ ] per unit volume [ $\text{L}^{-1}$ ]. At an  $\text{O}_2$  flow of 100  $\text{amol}\cdot\text{s}^{-1}\cdot\text{cell}^{-1}$  and a cell density of  $10^9 \text{ cells}\cdot\text{L}^{-1}$  ( $10^6 \text{ cells}\cdot\text{mL}^{-1}$ ), the volume-specific  $\text{O}_2$  flux is 100  $\text{nmol}\cdot\text{s}^{-1}\cdot\text{L}^{-1}$  (100  $\text{pmol}\cdot\text{s}^{-1}\cdot\text{mL}^{-1}$ ).


ET-capacity in human cell types including HEK 293, primary HUVEC and fibroblasts ranges from 50 to 180  $\text{amol}\cdot\text{s}^{-1}\cdot\text{cell}^{-1}$ , measured in intact cells in the noncoupled state (see Gnaiger 2014). At 100  $\text{amol}\cdot\text{s}^{-1}\cdot\text{cell}^{-1}$  corrected for *Rox*, the current across the mt-membranes,

$I_{H^+e}$ , approximates 193 pA·cell<sup>-1</sup> or 0.2 nA per cell. See Rich (2003) for an extension of quantitative bioenergetics from the molecular to the human scale, with a transmembrane proton flux equivalent to 520 A in an adult at a catabolic power of -110 W. Modelling approaches illustrate the link between protonmotive force and currents (Willis *et al.* 2016).

**Table 7. Conversion of units with preservation of numerical values.**

Name	Frequently used unit	Equivalent unit	Note
volume-specific flux, $J_{V,O_2}$	pmol·s <sup>-1</sup> ·mL <sup>-1</sup>	nmol·s <sup>-1</sup> ·L <sup>-1</sup>	1
	mmol·s <sup>-1</sup> ·L <sup>-1</sup>	mol·s <sup>-1</sup> ·m <sup>-3</sup>	
cell-specific flow, $I_{O_2/cell}$	pmol·s <sup>-1</sup> ·10 <sup>-6</sup> cells	amol·s <sup>-1</sup> ·cell <sup>-1</sup>	2
	pmol·s <sup>-1</sup> ·10 <sup>-9</sup> cells	zmol·s <sup>-1</sup> ·cell <sup>-1</sup>	3
cell number concentration, $C_{Nce}$	10 <sup>6</sup> cells·mL <sup>-1</sup>	10 <sup>9</sup> cells·L <sup>-1</sup>	
mitochondrial protein concentration, $C_{mtE}$	0.1 mg·mL <sup>-1</sup>	0.1 g·L <sup>-1</sup>	
mass-specific flux, $J_{O_2/m}$	pmol·s <sup>-1</sup> ·mg <sup>-1</sup>	nmol·s <sup>-1</sup> ·g <sup>-1</sup>	4
catabolic power, $P_k$	μW·10 <sup>-6</sup> cells	pW·cell <sup>-1</sup>	1
Volume	1,000 L	m <sup>3</sup> (1,000 kg)	
	L	dm <sup>3</sup> (kg)	
	mL	cm <sup>3</sup> (g)	
	μL	mm <sup>3</sup> (mg)	
	fL	μm <sup>3</sup> (pg)	5
amount of substance concentration	M = mol·L <sup>-1</sup>	mol·dm <sup>-3</sup>	

- 1208  
1209 1 pmol: picomole = 10<sup>-12</sup> mol 4 nmol: nanomole = 10<sup>-9</sup> mol  
1210 2 amol: attomole = 10<sup>-18</sup> mol 5 fL: femtolitre = 10<sup>-15</sup> L  
1211 3 zmol: zeptomole = 10<sup>-21</sup> mol  
1212  
1213

 We consider isolated mitochondria as powerhouses and proton pumps as molecular machines to relate experimental results to energy metabolism of the intact cell. The cellular P»/O<sub>2</sub> based on oxidation of glycogen is increased by the glycolytic (fermentative) substrate-level phosphorylation of 3 P»/Glyc or 0.5 mol P» for each mol O<sub>2</sub> consumed in the complete oxidation of a mol glycosyl unit (Glyc). Adding 0.5 to the mitochondrial P»/O<sub>2</sub> ratio of 5.4 yields a bioenergetic cell physiological P»/O<sub>2</sub> ratio close to 6. Two NADH equivalents are formed during glycolysis and transported from the cytosol into the mitochondrial matrix, either by the malate-aspartate shuttle or by the glycerophosphate shuttle resulting in different theoretical yields of ATP generated by mitochondria, the energetic cost of which potentially must be taken into account. Considering also substrate-level phosphorylation in the TCA cycle, this high P»/O<sub>2</sub> ratio not only reflects proton translocation and OXPHOS studied in isolation, but integrates mitochondrial physiology with energy transformation in the living cell (Gnaiger 1993a).

#### 4. Conclusions

MitoEAGLE can serve as a gateway to better diagnose mitochondrial respiratory defects linked to genetic variation, age-related health risks, sex-specific mitochondrial performance, lifestyle with its effects on degenerative diseases, and thermal and chemical environment. The present recommendations on coupling control states and rates, linked to the concept of the



protonmotive force, are focused on studies with mitochondrial preparations. These will be extended in a series of reports on pathway control of mitochondrial respiration, respiratory states in intact cells, and harmonization of experimental procedures.

The optimal choice for expressing mitochondrial and cell respiration (**Box 3**) as O<sub>2</sub> flow per biological system, and normalization for specific tissue-markers (volume, mass, protein) and mitochondrial markers (volume, protein, content, mtDNA, activity of marker enzymes, respiratory reference state) is guided by the scientific question under study. Interpretation of the obtained data depends critically on appropriate normalization, and therefore reporting rates merely as nmol·s<sup>-1</sup> is discouraged, since it restricts the analysis to intra-experimental comparison of relative (qualitative) differences. Expressing O<sub>2</sub> consumption per cell may not be possible when dealing with tissues. For studies with mitochondrial preparations, we recommend that normalizations be provided as far as possible: (1) on a per cell basis as O<sub>2</sub> flow (a biophysical normalization); (2) per g cell or tissue protein, or per cell or tissue mass as mass-specific O<sub>2</sub> flux (a cellular normalization); and (3) per mitochondrial marker as mt-specific flux (a mitochondrial normalization). With information on cell size and the use of multiple normalizations, maximum potential information is available (Renner *et al.* 2003; Wagner *et al.* 2011; Gnaiger 2014).

Total mitochondrial protein is frequently applied as a mitochondrial marker restricted to isolated mitochondria. The mitochondrial recovery and yield, and experimental criteria for evaluation of purity versus integrity should be reported. Mitochondrial markers—such as citrate synthase activity as an enzymatic matrix marker—provide a link to the tissue of origin on the basis of calculating the mitochondrial recovery, *i.e.*, the fraction of mitochondrial marker obtained from a unit mass of tissue.

---

### Box 3: Mitochondrial and cell respiration

---

Mitochondrial and cell respiration is the process of exergonic and exothermic energy transformation in which scalar redox reactions are coupled to vectorial ion translocation across a semipermeable membrane, which separates the small volume of a bacterial cell or mitochondrion from the larger volume of its surroundings. The electrochemical exergy can be partially conserved in the phosphorylation of ADP to ATP or in ion pumping, or dissipated in an electrochemical short-circuit. Respiration is thus clearly distinguished from fermentation as the counterpart of cellular core energy metabolism. Respiration is separated in mitochondrial preparations from the partial contribution of fermentative pathways of the intact cell. Residual oxygen consumption—as measured after inhibition of mitochondrial electron transfer—does not belong to the class of catabolic reactions and is, therefore, subtracted from total oxygen consumption to obtain baseline-corrected respiration.

---

Terms and symbols are summarized in **Table 8**. Their use will facilitate transdisciplinary communication and support further developments towards a consistent theory of bioenergetics and mitochondrial physiology. Technical terms related to and defined with normal words can be used as index terms in databases, support the creation of ontologies towards semantic information processing (MitoPedia), and help in communicating analytical findings as impactful data-driven stories. ‘*Making data available without making it understandable may be worse than not making it available at all*’ (National Academies of Sciences, Engineering, and Medicine 2018). This is a call to carefully contribute to FAIR principles (Findable, Accessible, Interoperable, Reusable) for the sharing of scientific data.

**Table 8. Terms, symbols, and units.**

Term	Symbol	Unit	Links and comments
alternative quinol oxidase	AOX		Fig. 1
amount of substance B	$n_B$	[mol]	
Complexes I to IV	CI to CIV		respiratory ET Complexes; Fig. 1
concentration of substance B	$c_B = n_B \cdot V^{-1}$ ; [B]	[mol·m <sup>-3</sup> ]	Box 2
electron transfer system	ETS		Fig. 1, Fig. 4
flow, for substance B	$I_B$	[mol·s <sup>-1</sup> ]	system-related extensive quantity; Fig. 6
flux, for substance B	$J_B$	<i>varies</i>	size-specific quantity; Fig. 6
inorganic phosphate	P <sub>i</sub>		Fig. 2
LEAK	LEAK		Tab. 1, Fig. 4
mass of sample X	$m_X$	[kg]	Tab. 4
mass of entity X	$M_X$	[kg]	mass of object X; Tab. 4
MITOCARTA			<a href="https://www.broadinstitute.org/scientific-community/science/programs/metabolic-disease-program/publications/mitocarta/mitocarta-in-0">https://www.broadinstitute.org/scientific-community/science/programs/metabolic-disease-program/publications/mitocarta/mitocarta-in-0</a>
MitoPedia			<a href="http://www.bioblast.at/index.php/MitoPedia">http://www.bioblast.at/index.php/MitoPedia</a>
mitochondria or mitochondrial	mt		Box 1
mitochondrial DNA	mtDNA		Box 1
mitochondrial concentration	$C_{mtE} = mtE \cdot V^{-1}$	[mtEU·m <sup>-3</sup> ]	Tab. 4
mitochondrial content	$mtE_X = mtE \cdot N_X^{-1}$	[mtEU·x <sup>-1</sup> ]	Tab. 4
mitochondrial elemental unit	mtEU	<i>varies</i>	Tab. 4, specific units for mt-marker
mitochondrial inner membrane	mtIM		MIM is widely used; the first M is replaced by mt; Box 1
mitochondrial outer membrane	mtOM		MOM is widely used; the first M is replaced by mt; Box 1
mitochondrial recovery	$Y_{mtE}$		fraction of <i>mtE</i> recovered in sample from the tissue of origin
mitochondrial yield	$Y_{mtE/m}$		$Y_{mtE/m} = Y_{mtE} \cdot D_{mtE}$
negative	neg		Fig. 2
number concentration of X	$C_{NX}$	[x·m <sup>-3</sup> ]	Tab. 4
number of entities X	$N_X$	[x]	Tab. 4, Fig. 7
number of entity B	$N_B$	[x]	Tab. 4
oxidative phosphorylation	OXPPOS		Tab. 1, Fig. 4
oxygen concentration	$c_{O_2} = n_{O_2} \cdot V^{-1}$ ; [O <sub>2</sub> ]	[mol·m <sup>-3</sup> ]	Section 3.2
phosphorylation of ADP to ATP	P <sub>»</sub>		Section 2.2
positive	pos		Fig. 2
proton in the negative compartment	H <sup>+</sup> <sub>neg</sub>		Fig. 2
proton in the positive compartment	H <sup>+</sup> <sub>pos</sub>		Fig. 2
rate of electron transfer in ET state	$E$		ET-capacity; Tab. 1
rate of LEAK respiration	$L$		Tab. 1
rate of oxidative phosphorylation	$P$		OXPPOS capacity; Tab. 1
rate of residual oxygen consumption	$R_{ox}$		Tab. 1
residual oxygen consumption	ROX		Tab. 1
specific mitochondrial density	$D_{mtE} = mtE \cdot m_X^{-1}$	[mtEU·kg <sup>-1</sup> ]	Tab. 7
volume	$V$	[m <sup>3</sup> ]	
weight, dry weight	$W_d$	[kg]	used as mass of sample X; Fig. 6
weight, wet weight	$W_w$	[kg]	used as mass of sample X; Fig. 6

**Acknowledgements**

We thank M. Beno for management assistance. Supported by COST Action CA15203 MitoEAGLE and K-Regio project MitoFit (E.G.).

**Competing financial interests:** E.G. is founder and CEO of Oroboros Instruments, Innsbruck, Austria.

## 5. References

- Altmann R (1894) Die Elementarorganismen und ihre Beziehungen zu den Zellen. Zweite vermehrte Auflage. Verlag Von Veit & Comp, Leipzig:160 pp.
- Beard DA (2005) A biophysical model of the mitochondrial respiratory system and oxidative phosphorylation. *PLoS Comput Biol* 1(4):e36.
- Benda C (1898) Weitere Mitteilungen über die Mitochondria. *Verh Dtsch Physiol Ges*:376-83.
- Birkedal R, Laasmaa M, Vendelin M (2014) The location of energetic compartments affects energetic communication in cardiomyocytes. *Front Physiol* 5:376.
- Breton S, Beaupré HD, Stewart DT, Hoeh WR, Blier PU (2007) The unusual system of doubly uniparental inheritance of mtDNA: isn't one enough? *Trends Genet* 23:465-74.
- Brown GC (1992) Control of respiration and ATP synthesis in mammalian mitochondria and cells. *Biochem J* 284:1-13.
- Calvo SE, Klauser CR, Mootha VK (2016) MitoCarta2.0: an updated inventory of mammalian mitochondrial proteins. *Nucleic Acids Research* 44:D1251-7.
- Calvo SE, Julien O, Clauser KR, Shen H, Kamer KJ, Wells JA, Mootha VK (2017) Comparative analysis of mitochondrial N-termini from mouse, human, and yeast. *Mol Cell Proteomics* 16:512-23.
- Campos JC, Queliconi BB, Bozi LHM, Bechara LRG, Dourado PMM, Andres AM, Jannig PR, Gomes KMS, Zambelli VO, Rocha-Resende C, Guatimosim S, Brum PC, Mochly-Rosen D, Gottlieb RA, Kowaltowski AJ, Ferreira JCB (2017) Exercise reestablishes autophagic flux and mitochondrial quality control in heart failure. *Autophagy* 13:1304-317.
- Canton M, Luvisetto S, Schmehl I, Azzone GF (1995) The nature of mitochondrial respiration and discrimination between membrane and pump properties. *Biochem J* 310:477-81.
- Chance B, Williams GR (1955a) Respiratory enzymes in oxidative phosphorylation. I. Kinetics of oxygen utilization. *J Biol Chem* 217:383-93.
- Chance B, Williams GR (1955b) Respiratory enzymes in oxidative phosphorylation: III. The steady state. *J Biol Chem* 217:409-27.
- Chance B, Williams GR (1955c) Respiratory enzymes in oxidative phosphorylation. IV. The respiratory chain. *J Biol Chem* 217:429-38.
- Chance B, Williams GR (1956) The respiratory chain and oxidative phosphorylation. *Adv Enzymol Relat Subj Biochem* 17:65-134.
- Cobb LJ, Lee C, Xiao J, Yen K, Wong RG, Nakamura HK, Mehta HH, Gao Q, Ashur C, Huffman DM, Wan J, Muzumdar N, Barzilai N, Cohen P (2016) Naturally occurring mitochondrial-derived peptides are age-dependent regulators of apoptosis, insulin sensitivity, and inflammatory markers. *Aging (Albany NY)* 8:796-809.
- Cohen ER, Cvitas T, Frey JG, Holmström B, Kuchitsu K, Marquardt R, Mills I, Pavese F, Quack M, Stohner J, Strauss HL, Takami M, Thor HL (2008) Quantities, units and symbols in physical chemistry, IUPAC Green Book, 3rd Edition, 2nd Printing, IUPAC & RSC Publishing, Cambridge.
- Cooper H, Hedges LV, Valentine JC, eds (2009) The handbook of research synthesis and meta-analysis. Russell Sage Foundation.
- Coopersmith J (2010) Energy, the subtle concept. The discovery of Feynman's blocks from Leibnitz to Einstein. Oxford University Press:400 pp.
- Cummins J (1998) Mitochondrial DNA in mammalian reproduction. *Rev Reprod* 3:172-82.
- Dai Q, Shah AA, Garde RV, Yonish BA, Zhang L, Medvitz NA, Miller SE, Hansen EL, Dunn CN, Price TM (2013) A truncated progesterone receptor (PR-M) localizes to the mitochondrion and controls cellular respiration. *Mol Endocrinol* 27:741-53.
- Divakaruni AS, Brand MD (2011) The regulation and physiology of mitochondrial proton leak. *Physiology (Bethesda)* 26:192-205.
- Doerrier C, Garcia-Souza LF, Krumschnabel G, Wohlfarter Y, Mészáros AT, Gnaiger E (2018) High-Resolution FluoRespirometry and OXPHOS protocols for human cells, permeabilized fibres from small biopsies of muscle and isolated mitochondria. *Methods Mol. Biol.* (in press)
- Doskey CM, van 't Erve TJ, Wagner BA, Buettner GR (2015) Moles of a substance per cell is a highly informative dosing metric in cell culture. *PLOS ONE* 10:e0132572.
- Drahota Z, Milerová M, Stieglerová A, Houstek J, Ostádal B (2004) Developmental changes of cytochrome c oxidase and citrate synthase in rat heart homogenate. *Physiol Res* 53:119-22.
- Duarte FV, Palmeira CM, Rolo AP (2014) The role of microRNAs in mitochondria: small players acting wide. *Genes (Basel)* 5:865-86.

- 1408 Ernster L, Schatz G (1981) Mitochondria: a historical review. *J Cell Biol* 91:227s-55s.
- 1409 Estabrook RW (1967) Mitochondrial respiratory control and the polarographic measurement of ADP:O ratios.
- 1410 *Methods Enzymol* 10:41-7.
- 1411 Faber C, Zhu ZJ, Castellino S, Wagner DS, Brown RH, Peterson RA, Gates L, Barton J, Bickett M, Hagerty L,
- 1412 Kimbrough C, Sola M, Bailey D, Jordan H, Elangbam CS (2014) Cardiolipin profiles as a potential
- 1413 biomarker of mitochondrial health in diet-induced obese mice subjected to exercise, diet-restriction and
- 1414 ephedrine treatment. *J Appl Toxicol* 34:1122-9.
- 1415 Fell D (1997) Understanding the control of metabolism. Portland Press.
- 1416 Garlid KD, Beavis AD, Ratkje SK (1989) On the nature of ion leaks in energy-transducing membranes. *Biochim*
- 1417 *Biophys Acta* 976:109-20.
- 1418 Garlid KD, Semrad C, Zinchenko V. Does redox slip contribute significantly to mitochondrial respiration? In:
- 1419 Schuster S, Rigoulet M, Ouhabi R, Mazat J-P, eds (1993) Modern trends in biothermokinetics. Plenum Press,
- 1420 New York, London:287-93.
- 1421 Gerö D, Szabo C (2016) Glucocorticoids suppress mitochondrial oxidant production via upregulation of
- 1422 uncoupling protein 2 in hyperglycemic endothelial cells. *PLoS One* 11:e0154813.
- 1423 Gnaiger E. Efficiency and power strategies under hypoxia. Is low efficiency at high glycolytic ATP production a
- 1424 paradox? In: Surviving Hypoxia: Mechanisms of Control and Adaptation. Hochachka PW, Lutz PL, Sick T,
- 1425 Rosenthal M, Van den Thillart G, eds (1993a) CRC Press, Boca Raton, Ann Arbor, London, Tokyo:77-109.
- 1426 Gnaiger E (1993b) Nonequilibrium thermodynamics of energy transformations. *Pure Appl Chem* 65:1983-2002.
- 1427 Gnaiger E (2001) Bioenergetics at low oxygen: dependence of respiration and phosphorylation on oxygen and
- 1428 adenosine diphosphate supply. *Respir Physiol* 128:277-97.
- 1429 Gnaiger E (2009) Capacity of oxidative phosphorylation in human skeletal muscle. New perspectives of
- 1430 mitochondrial physiology. *Int J Biochem Cell Biol* 41:1837-45.
- 1431 Gnaiger E (2014) Mitochondrial pathways and respiratory control. An introduction to OXPHOS analysis. 4th ed.
- 1432 *Mitochondr Physiol Network* 19.12. Oroboros MiPNet Publications, Innsbruck:80 pp.
- 1433 Gnaiger E, Méndez G, Hand SC (2000) High phosphorylation efficiency and depression of uncoupled respiration
- 1434 in mitochondria under hypoxia. *Proc Natl Acad Sci USA* 97:11080-5.
- 1435 Greggio C, Jha P, Kulkarni SS, Lagarrigue S, Broskey NT, Boutant M, Wang X, Conde Alonso S, Ofori E,
- 1436 Auwerx J, Cantó C, Amati F (2017) Enhanced respiratory chain supercomplex formation in response to
- 1437 exercise in human skeletal muscle. *Cell Metab* 25:301-11.
- 1438 Hinkle PC (2005) P/O ratios of mitochondrial oxidative phosphorylation. *Biochim Biophys Acta* 1706:1-11.
- 1439 Hofstadter DR (1979) Gödel, Escher, Bach: An eternal golden braid. A metaphorical fugue on minds and
- 1440 machines in the spirit of Lewis Carroll. Harvester Press:499 pp.
- 1441 Illaste A, Laasmaa M, Peterson P, Vendelin M (2012) Analysis of molecular movement reveals latticelike
- 1442 obstructions to diffusion in heart muscle cells. *Biophys J* 102:739-48.
- 1443 Jasienski M, Bazzaz FA (1999) The fallacy of ratios and the testability of models in biology. *Oikos* 84:321-26.
- 1444 Jepihhina N, Beraud N, Sepp M, Birkedal R, Vendelin M (2011) Permeabilized rat cardiomyocyte response
- 1445 demonstrates intracellular origin of diffusion obstacles. *Biophys J* 101:2112-21.
- 1446 Klepinin A, Ounpuu L, Guzun R, Chekulayev V, Timohhina N, Tepp K, Shevchuk I, Schlattner U, Kaambre T
- 1447 (2016) Simple oxygraphic analysis for the presence of adenylate kinase 1 and 2 in normal and tumor cells. *J*
- 1448 *Bioenerg Biomembr* 48:531-48.
- 1449 Klingenberg M (2017) UCP1 - A sophisticated energy valve. *Biochimie* 134:19-27.
- 1450 Koit A, Shevchuk I, Ounpuu L, Klepinin A, Chekulayev V, Timohhina N, Tepp K, Puurand M, Truu L, Heck K,
- 1451 Valvere V, Guzun R, Kaambre T (2017) Mitochondrial respiration in human colorectal and breast cancer
- 1452 clinical material is regulated differently. *Oxid Med Cell Longev* 1372640.
- 1453 Komlódi T, Tretter L (2017) Methylene blue stimulates substrate-level phosphorylation catalysed by succinyl-
- 1454 CoA ligase in the citric acid cycle. *Neuropharmacology* 123:287-98.
- 1455 Lane N (2005) Power, sex, suicide: mitochondria and the meaning of life. Oxford University Press:354 pp.
- 1456 Larsen S, Nielsen J, Neigaard Nielsen C, Nielsen LB, Wibrand F, Stride N, Schroder HD, Boushel RC, Helge
- 1457 JW, Dela F, Hey-Mogensen M (2012) Biomarkers of mitochondrial content in skeletal muscle of healthy
- 1458 young human subjects. *J Physiol* 590:3349-60.
- 1459 Lee C, Zeng J, Drew BG, Sallam T, Martin-Montalvo A, Wan J, Kim SJ, Mehta H, Hevener AL, de Cabo R,
- 1460 Cohen P (2015) The mitochondrial-derived peptide MOTS-c promotes metabolic homeostasis and reduces
- 1461 obesity and insulin resistance. *Cell Metab* 21:443-54.
- 1462 Lee SR, Kim HK, Song IS, Youm J, Dizon LA, Jeong SH, Ko TH, Heo HJ, Ko KS, Rhee BD, Kim N, Han J
- 1463 (2013) Glucocorticoids and their receptors: insights into specific roles in mitochondria. *Prog Biophys Mol*
- 1464 *Biol* 112:44-54.
- 1465 Leek BT, Mudaliar SR, Henry R, Mathieu-Costello O, Richardson RS (2001) Effect of acute exercise on citrate
- 1466 synthase activity in untrained and trained human skeletal muscle. *Am J Physiol Regul Integr Comp Physiol*
- 1467 *280*:R441-7.
- 1468 Lemieux H, Blier PU, Gnaiger E (2017) Remodeling pathway control of mitochondrial respiratory capacity by
- 1469 temperature in mouse heart: electron flow through the Q-junction in permeabilized fibers. *Sci Rep* 7:2840.



- 1470 Lenaz G, Tioli G, Falasca AI, Genova ML (2017) Respiratory supercomplexes in mitochondria. In: Mechanisms  
1471 of primary energy trasduction in biology. M Wikstrom (ed) Royal Society of Chemistry Publishing, London,  
1472 UK:296-337.
- 1473 Margulis L (1970) Origin of eukaryotic cells. New Haven: Yale University Press.
- 1474 Meinild Lundby AK, Jacobs RA, Gehrig S, de Leur J, Hauser M, Bonne TC, Flück D, Dandanell S, Kirk N,  
1475 Kaech A, Ziegler U, Larsen S, Lundby C (2018) Exercise training increases skeletal muscle mitochondrial  
1476 volume density by enlargement of existing mitochondria and not de novo biogenesis. *Acta Physiol* 222,  
1477 e12905.
- 1478 Menshikova EV, Ritov VB, Fairfull L, Ferrell RE, Kelley DE, Goodpaster BH (2006) Effects of exercise on  
1479 mitochondrial content and function in aging human skeletal muscle. *J Gerontol A Biol Sci Med Sci* 61:534-  
1480 40.
- 1481 Menshikova EV, Ritov VB, Ferrell RE, Azuma K, Goodpaster BH, Kelley DE (2007) Characteristics of skeletal  
1482 muscle mitochondrial biogenesis induced by moderate-intensity exercise and weight loss in obesity. *J Appl*  
1483 *Physiol* (1985) 103:21-7.
- 1484 Menshikova EV, Ritov VB, Toledo FG, Ferrell RE, Goodpaster BH, Kelley DE (2005) Effects of weight loss  
1485 and physical activity on skeletal muscle mitochondrial function in obesity. *Am J Physiol Endocrinol Metab*  
1486 288:E818-25.
- 1487 Miller GA (1991) The science of words. Scientific American Library New York:276 pp.
- 1488 Mitchell P (1961) Coupling of phosphorylation to electron and hydrogen transfer by a chemi-osmotic type of  
1489 mechanism. *Nature* 191:144-8.
- 1490 Mitchell P (2011) Chemiosmotic coupling in oxidative and photosynthetic phosphorylation. *Biochim Biophys*  
1491 *Acta Bioenergetics* 1807:1507-38.
- 1492 Mogensen M, Sahlin K, Fernström M, Glintborg D, Vind BF, Beck-Nielsen H, Højlund K (2007) Mitochondrial  
1493 respiration is decreased in skeletal muscle of patients with type 2 diabetes. *Diabetes* 56:1592-9.
- 1494 Mohr PJ, Phillips WD (2015) Dimensionless units in the SI. *Metrologia* 52:40-7.
- 1495 Moreno M, Giacco A, Di Munno C, Goglia F (2017) Direct and rapid effects of 3,5-diiodo-L-thyronine (T2).  
1496 *Mol Cell Endocrinol* 7207:30092-8.
- 1497 Morrow RM, Picard M, Derbeneva O, Leipzig J, McManus MJ, Gouspillou G, Barbat-Artigas S, Dos Santos C,  
1498 Hepple RT, Murdock DG, Wallace DC (2017) Mitochondrial energy deficiency leads to hyperproliferation of  
1499 skeletal muscle mitochondria and enhanced insulin sensitivity. *Proc Natl Acad Sci U S A* 114:2705-10.
- 1500 Murley A, Nunnari J (2016) The emerging network of mitochondria-organelle contacts. *Mol Cell* 61:648-53.
- 1501 National Academies of Sciences, Engineering, and Medicine (2018) International coordination for science data  
1502 infrastructure: Proceedings of a workshop—in brief. Washington, DC: The National Academies Press. doi:  
1503 <https://doi.org/10.17226/25015>.
- 1504 Paradies G, Paradies V, De Benedictis V, Ruggiero FM, Petrosillo G (2014) Functional role of cardiolipin in  
1505 mitochondrial bioenergetics. *Biochim Biophys Acta* 1837:408-17.
- 1506 Pesta D, Gnaiger E (2012) High-Resolution Respirometry. OXPHOS protocols for human cells and  
1507 permeabilized fibres from small biopsies of human muscle. *Methods Mol Biol* 810:25-58.
- 1508 Pesta D, Hoppel F, Macek C, Messner H, Faulhaber M, Kobel C, Parson W, Bartscher M, Schocke M, Gnaiger  
1509 E (2011) Similar qualitative and quantitative changes of mitochondrial respiration following strength and  
1510 endurance training in normoxia and hypoxia in sedentary humans. *Am J Physiol Regul Integr Comp Physiol*  
1511 301:R1078–87.
- 1512 Price TM, Dai Q (2015) The role of a mitochondrial progesterone receptor (PR-M) in progesterone action.  
1513 *Semin Reprod Med* 33:185-94.
- 1514 Puchowicz MA, Varnes ME, Cohen BH, Friedman NR, Kerr DS, Hoppel CL (2004) Oxidative phosphorylation  
1515 analysis: assessing the integrated functional activity of human skeletal muscle mitochondria – case studies.  
1516 *Mitochondrion* 4:377-85. Puntschart A, Claassen H, Jostardt K, Hoppeler H, Billeter R (1995) mRNAs of  
1517 enzymes involved in energy metabolism and mtDNA are increased in endurance-trained athletes. *Am J*  
1518 *Physiol* 269:C619-25.
- 1519 Quiros PM, Mottis A, Auwerx J (2016) Mitonuclear communication in homeostasis and stress. *Nat Rev Mol*  
1520 *Cell Biol* 17:213-26.
- 1521 Reichmann H, Hoppeler H, Mathieu-Costello O, von Bergen F, Pette D (1985) Biochemical and ultrastructural  
1522 changes of skeletal muscle mitochondria after chronic electrical stimulation in rabbits. *Pflügers Arch* 404:1-  
1523 9.
- 1524 Renner K, Amberger A, Konwalinka G, Gnaiger E (2003) Changes of mitochondrial respiration, mitochondrial  
1525 content and cell size after induction of apoptosis in leukemia cells. *Biochim Biophys Acta* 1642:115-23.
- 1526 Rich P (2003) Chemiosmotic coupling: The cost of living. *Nature* 421:583.
- 1527 Rostovtseva TK, Sheldon KL, Hassanzadeh E, Monge C, Saks V, Bezrukov SM, Sackett DL (2008) Tubulin  
1528 binding blocks mitochondrial voltage-dependent anion channel and regulates respiration. *Proc Natl Acad Sci*  
1529 *USA* 105:18746-51.

- 1530 Rustin P, Parfait B, Chretien D, Bourgeron T, Djouadi F, Bastin J, Rötig A, Munnich A (1996) Fluxes of  
1531 nicotinamide adenine dinucleotides through mitochondrial membranes in human cultured cells. *J Biol Chem*  
1532 271:14785-90.
- 1533 Saks VA, Veksler VI, Kuznetsov AV, Kay L, Sikk P, Tiivel T, Tranqui L, Olivares J, Winkler K, Wiedemann F,  
1534 Kunz WS (1998) Permeabilised cell and skinned fiber techniques in studies of mitochondrial function in  
1535 vivo. *Mol Cell Biochem* 184:81-100.
- 1536 Salabei JK, Gibb AA, Hill BG (2014) Comprehensive measurement of respiratory activity in permeabilized cells  
1537 using extracellular flux analysis. *Nat Protoc* 9:421-38.
- 1538 Sazanov LA (2015) A giant molecular proton pump: structure and mechanism of respiratory complex I. *Nat Rev*  
1539 *Mol Cell Biol* 16:375-88.
- 1540 Schneider TD (2006) Claude Shannon: biologist. The founder of information theory used biology to formulate  
1541 the channel capacity. *IEEE Eng Med Biol Mag* 25:30-3.
- 1542 Schönfeld P, Dymkowska D, Wojtczak L (2009) Acyl-CoA-induced generation of reactive oxygen species in  
1543 mitochondrial preparations is due to the presence of peroxisomes. *Free Radic Biol Med* 47:503-9.
- 1544 Schultz J, Wiesner RJ (2000) Proliferation of mitochondria in chronically stimulated rabbit skeletal muscle--  
1545 transcription of mitochondrial genes and copy number of mitochondrial DNA. *J Bioenerg Biomembr* 32:627-  
1546 34.
- 1547 Simson P, Jepihhina N, Laasmaa M, Peterson P, Birkedal R, Vendelin M (2016) Restricted ADP movement in  
1548 cardiomyocytes: Cytosolic diffusion obstacles are complemented with a small number of open mitochondrial  
1549 voltage-dependent anion channels. *J Mol Cell Cardiol* 97:197-203.
- 1550 Stucki JW, Ineichen EA (1974) Energy dissipation by calcium recycling and the efficiency of calcium transport  
1551 in rat-liver mitochondria. *Eur J Biochem* 48:365-75.
- 1552 Tonkonogi M, Harris B, Sahlin K (1997) Increased activity of citrate synthase in human skeletal muscle after a  
1553 single bout of prolonged exercise. *Acta Physiol Scand* 161:435-6.
- 1554 Waczulikova I, Habodaszova D, Cagalinec M, Ferko M, Ulicna O, Mateasik A, Sikurova L, Ziegelhöffer A  
1555 (2007) Mitochondrial membrane fluidity, potential, and calcium transients in the myocardium from acute  
1556 diabetic rats. *Can J Physiol Pharmacol* 85:372-81.
- 1557 Wagner BA, Venkataraman S, Buettner GR (2011) The rate of oxygen utilization by cells. *Free Radic Biol Med*  
1558 51:700-712.
- 1559 Wang H, Hiatt WR, Barstow TJ, Brass EP (1999) Relationships between muscle mitochondrial DNA content,  
1560 mitochondrial enzyme activity and oxidative capacity in man: alterations with disease. *Eur J Appl Physiol*  
1561 *Occup Physiol* 80:22-7.
- 1562 Watt IN, Montgomery MG, Runswick MJ, Leslie AG, Walker JE (2010) Bioenergetic cost of making an  
1563 adenosine triphosphate molecule in animal mitochondria. *Proc Natl Acad Sci U S A* 107:16823-7.
- 1564 Weibel ER, Hoppeler H (2005) Exercise-induced maximal metabolic rate scales with muscle aerobic capacity. *J*  
1565 *Exp Biol* 208:1635-44.
- 1566 White DJ, Wolff JN, Pierson M, Gemmell NJ (2008) Revealing the hidden complexities of mtDNA inheritance.  
1567 *Mol Ecol* 17:4925-42.
- 1568 Wikström M, Hummer G (2012) Stoichiometry of proton translocation by respiratory complex I and its  
1569 mechanistic implications. *Proc Natl Acad Sci U S A* 109:4431-6.
- 1570 Willis WT, Jackman MR, Messer JI, Kuzmiak-Glancy S, Glancy B (2016) A simple hydraulic analog model of  
1571 oxidative phosphorylation. *Med Sci Sports Exerc* 48:990-1000.